



Nonlinear viscoelasticity of incompressible isotropic solids

Jinlai Zhou, Gengchao Yang, Qinghe Yao*

School of Aeronautics and Astronautics, Sun Yat-sen University, Guangzhou 510275, China

ARTICLE INFO

Keywords:

Incompressible isotropic solids
Constitutive model
Boltzmann superposition principle
Relaxation modeling
Creep modeling
Boltzmann's equations

ABSTRACT

The development of isotropic nonlinear viscoelastic solid constitutive models constitutes an integral part of solid mechanics. In this work, a general constitutive behavior framework for nonlinear viscoelastic solid materials is developed via systematic stress relaxation and creep experiments on polypropylene (PP). Results indicate that the infinite hyperelastic-plastic constitutive behavior serves as the sole physical boundary for evaluating structural delayed stability. Thus, the threshold stress between low-stress creep stability and high-stress creep fracture of nonlinear viscoelastic solid is determined. It is revealed that the nonlinear viscoelastic constitutive behavior represents a convergence process from instantaneous hyperelasticity to infinite hyperelasticity. To fully characterize their relaxation and creep viscoelastic properties, we propose a novel architecture based on series-parallel combinations of hyperelastic springs and dampers. By integrating Maxwell and Kelvin linear viscoelastic theories with the incompressible Mooney-Rivlin hyperelastic model, we develop incompressible nonlinear viscoelastic stress relaxation and creep constitutive models. The developed models exhibit excellent predictive performance. Boltzmann's equations are derived based on the Boltzmann nonlinear superposition principle, revealing the constitutive relations for nonlinear solids. These equations establish a connection between special and generalized relaxation / creep constitutive behaviors. This research focuses on small deformations in incompressible solids, laying the groundwork for future investigations into large deformations in compressible solids.

1. Introduction

Computational solid mechanics, composed of numerical algorithms (predominantly the finite element method) and solid constitutive models, plays a pivotal role in engineering applications. This discipline is traditionally categorized into four major branches: linear elastic solids, linear viscoelastic solids, nonlinear elastic solids, and nonlinear viscoelastic solids.

The constitutive framework for linear elastic solids is formulated through the generalized Hooke's law, pioneered by Hooke and systematically developed by Cauchy, Young, Poisson, and subsequent researchers. This model finds extensive engineering utility in describing materials such as room-temperature metals [1].

The theoretical framework of linear viscoelastic solids was primarily developed during the 19th century, forming a mature system established by Maxwell, Kelvin, Boltzmann, and their contemporaries. The main contributions include Maxwell [2] determining the linear viscoelastic stress relaxation behavior (relaxation stress and constant strain are a linear constitutive relation) and establishing the Maxwell fluid model.

Kelvin characterized the linear viscoelastic creep response (creep strain and constant stress are a linear constitutive relation) and proposed the Kelvin solid model. Boltzmann [3] introduced the linear superposition principle, deriving constitutive equations that connect special (Fig. 1a) and generalized (Fig. 1b) static responses in linear solids [4]. These equations mathematically formalize the superposition law governing single-physical-field interactions in such materials. This well-established theory finds extensive engineering applications in modeling high-temperature metallic materials [1,5].

The systematic development of nonlinear elastic (hyperelastic) constitutive models occurred primarily during the 20th century. Key hyperelastic models include: Neo-Hookean [6], Mooney [7]-Rivlin [8], Blatz-Ko [9], Varga [10], Veronda-Westmann [11], Odgen [12], Arruda-Boyce [13], Yeoh [14], Gent [15] models, etc. Among these, the Mooney-Rivlin model based on strain tensor invariants and the Odgen model based on principal stretches are the main representatives. These models are widely adopted for engineering applications involving rubber-like materials [1].

The theoretical framework for nonlinear viscoelastic solids lagged

* Correspondence

E-mail address: yaoqhe@mail.sysu.edu.cn (Q. Yao).

<https://doi.org/10.1016/j.ijmecsci.2025.110330>

Received 15 January 2025; Received in revised form 25 March 2025; Accepted 29 April 2025

Available online 29 April 2025

0020-7403/© 2025 Elsevier Ltd. All rights reserved, including those for text and data mining, AI training, and similar technologies.

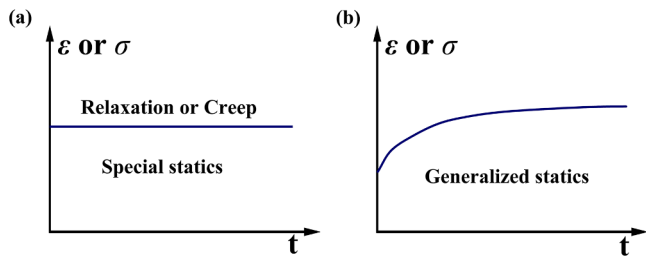


Fig. 1. The superposition of single physical fields in solid materials. (a). Special statics (Relaxation and creep loads). (b). Generalized statics (Generalized relaxation or creep loads).

behind, with systematic studies emerging more recently. Numerous experimental results indicate that the creep strain of nonlinear viscoelastic solid materials exhibits a nonlinear relation with constant stress. Extensive experimental evidence reveals the stress-dependent creep behavior, which is completely different from the linear viscoelastic constitutive relation. Biomaterials (e.g., periodontal ligament [16], cartilage [17], trabecular bone [18]) show decreasing creep compliance with increasing stress. Polymeric materials (e.g., PP [19]) exhibit increasing creep compliance under elevated stress. Polymeric materials, as typical nonlinear viscoelastic solid materials, are often used as matrices for composite materials. Widely used in industries such as water, oil and gas, aerospace, and chemical [20]. Notable contributions include Rafiee et al. [21–23], who developed multi-stage creep protocols to characterize long-term (over one year) nonlinear creep in composite materials. Zhou et al. [24] introduced the "anchored" concept, defining nonlinear viscoelastic behavior through relaxation modulus spectrum $G(\epsilon, t)$ and creep compliance spectrum $J(\sigma, t)$. Despite recent advancements, characterization of structural creep stability in nonlinear viscoelastic solids remains qualitative, with low-stress creep maintaining stability whereas high-stress creep induces fracture. The threshold stress between low stress creep stability and high stress creep fracture cannot be determined. The unresolved challenge lies in determining the critical stress threshold separating these regimes, fundamentally due to the lack of predictive constitutive behavior frameworks.

The earliest research on nonlinear theory of viscoelasticity was proposed by Rivlin and Ericksen [25] for the viscoelastic theory of isotropic solids. Early investigations into finite viscoelasticity [26–28] were primarily based on memory decay theories [29–32]. Power-law functions were adopted in some studies to model nonlinear viscoelastic creep behavior [33–35]. However, mathematical convergence issues inherent to power-law representations of creep strain have limited their theoretical rigor. Currently, no universally accepted constitutive models exist for describing both relaxation and creep phenomena in nonlinear viscoelastic solids.

The understanding of nonlinear solid responses to generalized static loads remains incomplete. Key contributions include: Green and Rivlin [29] developed numerical approximation equations extending Boltzmann's linear superposition principle to nonlinear solids. Ward et al. [36] proposed computational methods for multi-stage step loadings. Fung [37,38] introduced the quasi-linear viscoelastic (QLV) theory, widely applied to biological soft tissues. Schapery [39] formulated a nonlinear thermo-viscoelastic theory within irreversible thermodynamics. Zhou et al. [24] advanced the Boltzmann nonlinear superposition principle, postulating nonlinear constitutive relations for single-physical-field interactions in solids. Notably, experimental validation of these nonlinear superposition relations remains lacking. Furthermore, no unified analytical equations exist to bridge the gap between special (Fig. 1a) and generalized (Fig. 1b) static responses in nonlinear solids, representing a significant theoretical deficit.

This work explores the nonlinear viscoelastic constitutive behavior of typical nonlinear viscoelastic solid material PP through a series of experiments (quasi-static tensile test, stress relaxation test, and creep

test), and establishes a general constitutive behavior framework for nonlinear viscoelastic solids. We established Maxwell-Mooney-Rivlin fluid relaxation and Kelvin-Mooney-Rivlin solid creep nonlinear viscoelastic constitutive models. Based on the Boltzmann nonlinear superposition principle, the Boltzmann's equations is derived, which reveals the single physical field superposition constitutive relation of nonlinear solid materials.

2. Materials and methods

Section 2 introduces the experimental setup, including material preparation and experimental methods. To validate the proposed general constitutive behavior framework, nonlinear viscoelastic stress relaxation and creep models, Boltzmann nonlinear superposition relations, and corresponding equations. A series of static, stress relaxation, creep (recovery), and generalized relaxation / creep tensile experiments were performed on representative isotropic polymeric samples.

2.1. Preparation of specimens

PP [19,36] is chosen as the model material due to its wide range of applications and excellent mechanical properties. The sample measures 90mm in length, 10mm in width, and 4mm in thickness. The experimental instrument adopts an Division of ITW Limited (UK) 10KN material testing machine with a model of Instron/68TM-10. The displacement resolution of the instrument is 0.001mm. The force resolution is 0.001N, and the accuracy meets the experimental requirements (Fig. 2).

2.2. Experiment

Room-temperature experiments were performed using an Instron/68TM-10 universal testing machine, including strain-controlled static tensile tests, stress relaxation tests, and stress-controlled creep tests. A total of six test categories were conducted: 1 static tensile experiment (S1), 7 stress relaxation experiments (R2–R8), 5 creep experiments (C9–C13), 1 creep-recovery experiment (CR14), 1 generalized relaxation experiment (GR15), and 1 generalized creep experiment (GC16). The maximum quasi-static loading rate of 10^{-3} /s was employed to approximate theoretical step loading and minimize dynamic impacts and thermal effects. Prior to formal testing, a zero-stress creep protocol was applied to eliminate initial stresses. For stress relaxation tests, constant strains of 0.50 %, 0.75 %, 1.0 %, 2.0 %, 3.0 %, 4.0 %, and 5.0 % were imposed. Creep tests utilized constant stresses of 4 MPa, 6 MPa, 8 MPa, 15 MPa, and 20 MPa, with the creep-recovery experiment conducted at 10 MPa.

3. Experimental result

Section 3 introduces the key experimental results of PP. These include the special and generalized stress relaxation constitutive behavior, as well as the special and generalized creep constitutive behavior. It also defines the yield and fracture strength of nonlinear viscoelastic solids.

3.1. Stress relaxation constitutive behavior

The stress relaxation constitutive behavior was studied at constant strain levels of 0.50 %, 0.75 %, 1.0 %, 2.0 %, 3.0 %, 4.0 %, and 5.0 % at room temperature (Fig. 3). The instantaneous hyperelastic-plastic constitutive behavior occurs under step loading (Fig. 3a), and the instantaneous hyperelastic-plastic constitutive behavior determines the starting point of relaxation stress. The relaxation stress exhibits exponential decay and approaches constant stress after an infinite duration (Fig. 3b). During the relaxation process, the time-dependent viscous effect gradually disappears and converges to an infinite hyperelastic-

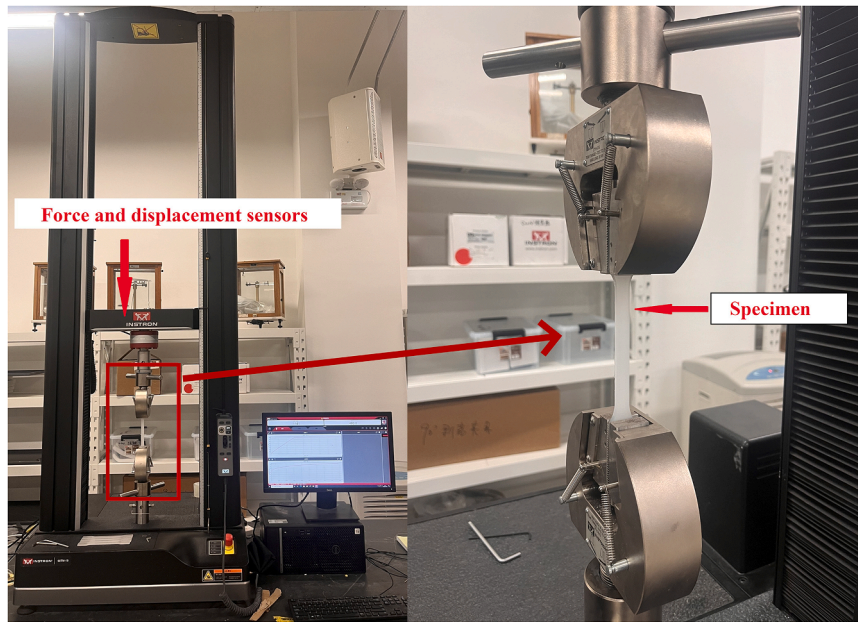


Fig. 2. The tensile test device of the polypropylene.

plastic boundary (Fig. 3c). Essentially, step loading stores hyperelastic strain energy. Under constant strain, the stress relaxation is only phenomenological and essentially viscous consumption of hyperelastic strain energy. From another perspective, stress relaxation constitutive behavior is the process of convergence from quasi-static unstable instantaneous hyperelastic-plastic boundary to static stable infinite hyperelastic-plastic boundary (Fig. 3d).

3.2. Creep constitutive behavior

The creep constitutive behavior was studied at constant stress levels of 4MPa, 6MPa, 8MPa, 15MPa, and 20MPa at room temperature (Fig. 4). An instantaneous hyperelastic-plastic response occurs under step loading (Fig. 4a), determining the initial point of creep deformation. The creep strain increases exponentially and approaches a constant value after an infinite period (Fig. 4b). During the creep process, the time-dependent viscous effect gradually disappears and converges to an infinite hyperelastic-plastic boundary (Fig. 4c). The essence of creep is the convergence from quasi-static unstable instantaneous hyperelastic-plastic boundary to statically stable infinite hyperelastic-plastic boundary (Fig. 4d). However, when the creep constant stress is greater than the infinite hyperelastic-plastic boundary, the creep strain cannot converge to the infinite hyperelastic-plastic boundary. The time-dependent viscous effect has always existed, and experimental results have demonstrated the Newtonian fluid characteristics (Fig. 4e). It has been proven from the perspective of creep that the constitutive behavior of infinite hyperelastic-plastic boundaries is the key to determining creep stability and fracture failure, and this physical stability is unique.

3.3. Yield strain and engineering allowable stress

The creep recovery constitutive behavior was studied at room temperature and a constant stress level of 10 MPa (Fig. 4f). After the creep strain of PP reached 1.5 %, it recovered about 1.3 % of the viscoelastic creep strain and retained about 0.2 % of the viscoplastic creep strain. Experiments have shown that the yield strain of PP is approximately 1.3 % (Fig. 3d). The constitutive behavior is considered viscoelastic when the strain is less than the yield strain, and viscoplastic when the strain is greater than the yield strain. The yield strength of PP is about 8MPa, and the fracture strength is about 13MPa (Fig. 3d). The creep constant stress

of PP is between 0-8MPa, which is viscoelastic creep, and the material remains stable (Fig. 4b). The creep constant stress of PP is between 8-13MPa, which is viscoelastic and viscoplastic creep, and the material remains stable. The creep constant stress of PP is greater than 13MPa, which is viscoelastic and viscoplastic creep. The material is unstable and leads to fracture (Fig. 4e).

3.4. Generalized nonlinear constitutive behavior

The relaxation stress and constant strain of linear viscoelastic materials have a linear constitutive relation, with the ratio being the relaxation modulus. The creep strain and constant stress have a linear constitutive relation, and the ratio is the creep compliance. PP exhibits significant nonlinear viscoelastic solid material properties. The relaxation modulus decreases with increasing constant strain (Fig. 5a), while the creep compliance increases with increasing constant stress (Fig. 5b). The generalized nonlinear relaxation test procedure is as follows: Step loading to 0.5 % for 10000s without change, then step loading to 0.75 % for 10000s without change, and then step loading to 1.0 % for 10000s without change (Fig. 6a). The generalized relaxation constitutive response of PP is shown in Fig. 6b. The generalized nonlinear creep test procedure is as follows: Step loading to 4MPa for 10000s without change, then step loading to 6MPa for 10000s without change, and then step loading to 8MPa for 10000s without change (Fig. 6c). The generalized creep constitutive response of PP is shown in Fig. 6d.

4. Constitutive behavior and models

The steps and methods of the present research are summarized in the scheme of Fig. 7. A brief description of each step is provided in the following. As is well known, the evolution of solid mechanics for linear elastic solids (Fig. 8a), linear viscoelastic solids (Fig. 8b), and nonlinear elastic solids (Fig. 8c) has historically been guided by experimentally observed objective constitutive behaviors. Subsequently, mathematical constitutive modeling is employed to accurately describe these behaviors, with numerical simulations enabling large-scale engineering applications. However, incomplete understanding of nonlinear viscoelastic solid behavior has resulted in the absence of a universally accepted theoretical framework for practical engineering implementation. Adhering to the classical methodology, we develop a unified constitutive

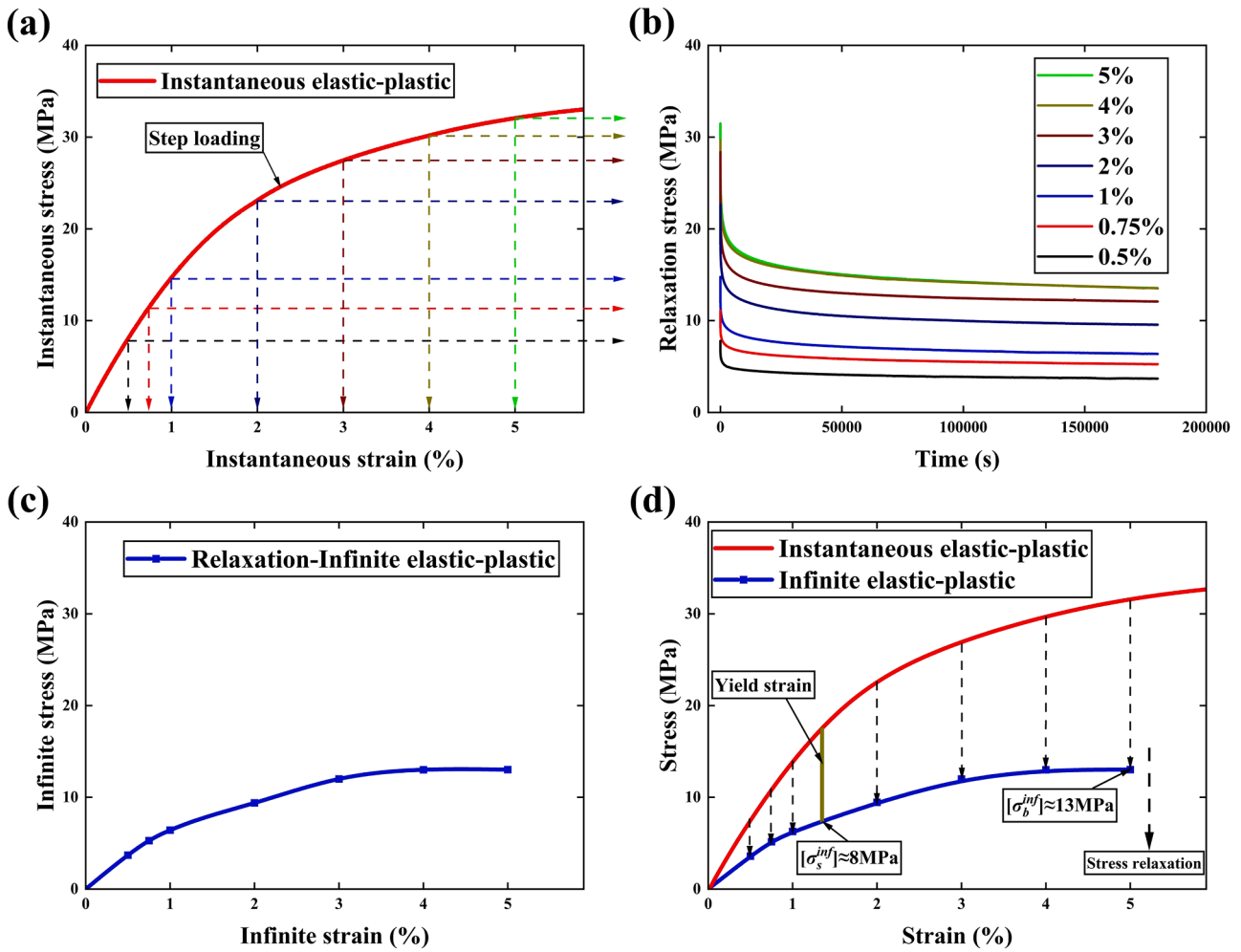


Fig. 3. The stress relaxation constitutive behavior of polypropylene. (a). Instantaneous hyperelastic-plastic constitutive behavior under step loading. The instantaneous hyperelastic-plastic constitutive behavior in Fig. 3a determines the starting point of the relaxation stress in Fig. 3b. (b). Stress relaxation occurs at constant strains of 0.50 %, 0.75 %, 1.0 %, 2.0 %, 3.0 %, 4.0 %, and 5.0 %. The stress of the relaxation stress curve in Fig. 3b converges to the infinite hyperelastic-plastic constitutive behavior in Fig. 3c. In linear constitutive theory, the relation between relaxation stress and constant strain is linear. The relaxation stress and constant strain of polypropylene exhibit a clear nonlinear constitutive relation. (c). The infinite hyperelastic-plastic constitutive behavior. (d). The instantaneous hyperelastic-plastic constitutive behavior undergoes stress relaxation and converges to infinite hyperelastic-plastic constitutive behavior.

framework for nonlinear viscoelastic solids based on PP experimental results. In addition, nonlinear viscoelastic stress relaxation and creep models are proposed, and finally, the Boltzmann superposition principle and its corresponding equations are derived to characterize the nonlinear superposition constitutive relations.

4.1. General constitutive behavior framework

Zhou et al. [5] experimentally demonstrated that linear elastic-plastic zones in metallic materials at room temperature (Fig. 8a) evolve into linear viscoelastic and viscoplastic zones at elevated temperatures (Fig. 8b). Temperature elevation is identified as the critical factor inducing time-dependent viscous effects in solid materials. Notably, nonlinear elastic solids such as rubber exhibit nonlinear viscoelastic behavior at high temperatures, while polymeric materials display nonlinear viscoelastic characteristics even at room temperature. Significantly, viscous effects in polymers can be suppressed by reducing temperature, indicating that time-independent elastic-plastic behavior (Fig. 8a & 8c) represents the limiting case of time-dependent viscoelastic-viscoplastic behavior (Fig. 8b & 8d). These two zones form a complementary relationship, interconvertible through temperature variations.

Step loading [16] is considered as a static load in an infinitesimal

time. In the instantaneous state, ‘time’ does not exist as a mathematical variable, and from a physical perspective, the viscous mechanics behavior requires ‘time’ to characterize. Nonlinear viscoelastic solid materials exhibit instantaneous hyperelastic-plastic constitutive behavior only under step loading ($t=0^+$). After step loading, time-dependent viscous effects lead to the emergence of viscoelastic and viscoplastic constitutive behaviors. After infinite time, the constitutive behavior converges to the statically stable boundary of infinite hyperelastic-plasticity. Zhou et al. [5] experimentally and theoretically demonstrated the absence of “viscoplastic stress relaxation” phenomenon, thereby establishing that the yield behavior of solid materials is solely strain-dependent, independent of stress (Fig. 8b).

Key boundary conditions defining the nonlinear viscoelastic zone include:

- Instantaneous hyperelastic behavior
- Infinite hyperelastic behavior
- Yield strain behavior

For the viscoplastic zone, critical boundaries are:

- Instantaneous plastic behavior
- Infinite plastic behavior

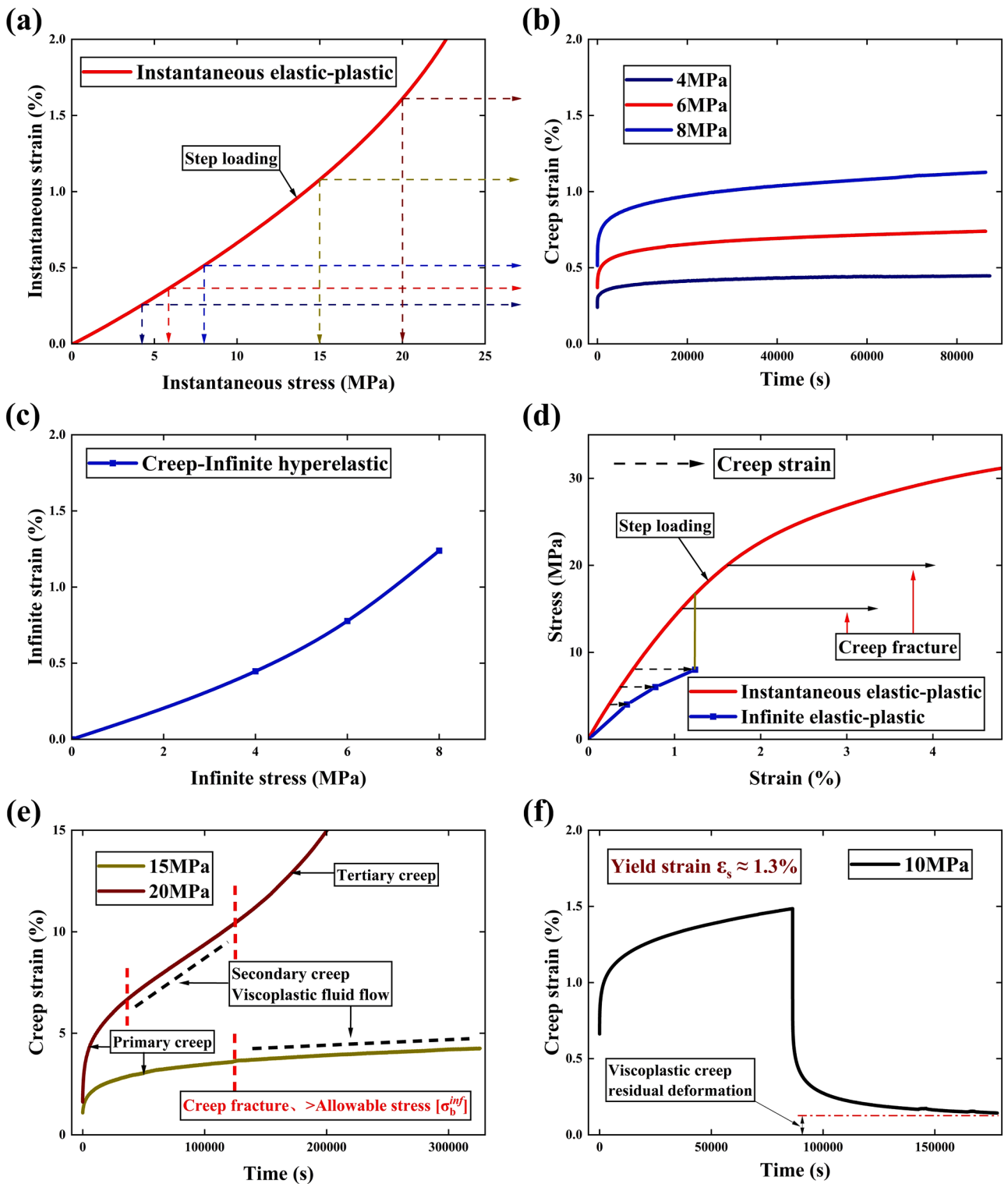


Fig. 4. The creep constitutive behavior of polypropylene. (a). Instantaneous hyperelastic-plastic constitutive behavior under step loading. The instantaneous hyperelastic-plastic in Fig. 4a determines the starting point of the creep strain in Fig. 4b. (b). Creep strain occurs at constant stress of 4MPa, 6MPa, and 8MPa. The strain of the creep strain in Fig. 4b converges to the infinite linear-elastic plastic constitutive behavior in Fig. 4c. In linear constitutive theory, the relationship between creep strain and constant stress is linear. The creep strain and constant stress of polypropylene exhibit a clear nonlinear constitutive relation. (c). The creep strain converges to an infinite hyperelastic-plastic constitutive behavior. (d). The instantaneous hyperelastic-plastic constitutive behavior undergoes creep strain and converges to infinite hyperelastic-plastic constitutive behavior. (e). Creep strain occurs at constant stress of 15MPa and 20MPa. The creep fracture constitutive behavior occurs. (f). Creep recovery experiment of polypropylene at 10MPa.

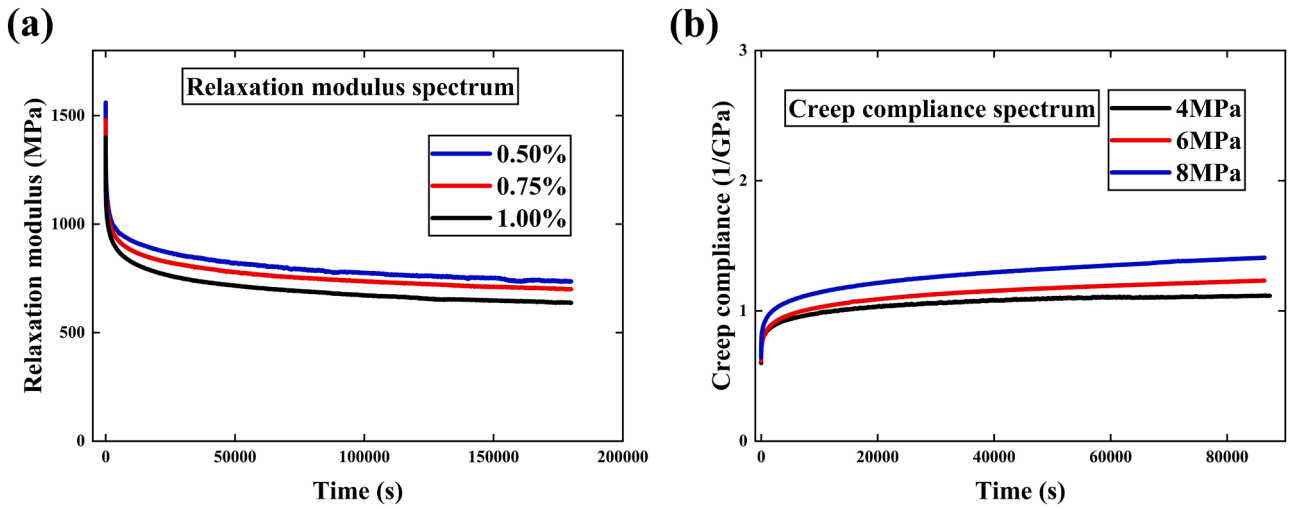


Fig. 5. Nonlinear viscoelastic relaxation modulus spectrum and creep compliance spectrum. (a). In a linear constitutive theory, the relaxation modulus is strain-independent. The relaxation modulus of polypropylene decreases with increasing constant strain. The relaxation modulus of nonlinear viscoelastic solids is strain-dependent. (b). In a linear constitutive theory, the creep compliance is stress-independent. The creep compliance of polypropylene increases with the increase of constant stress. The creep compliance of nonlinear viscoelastic solids is stress-dependent.

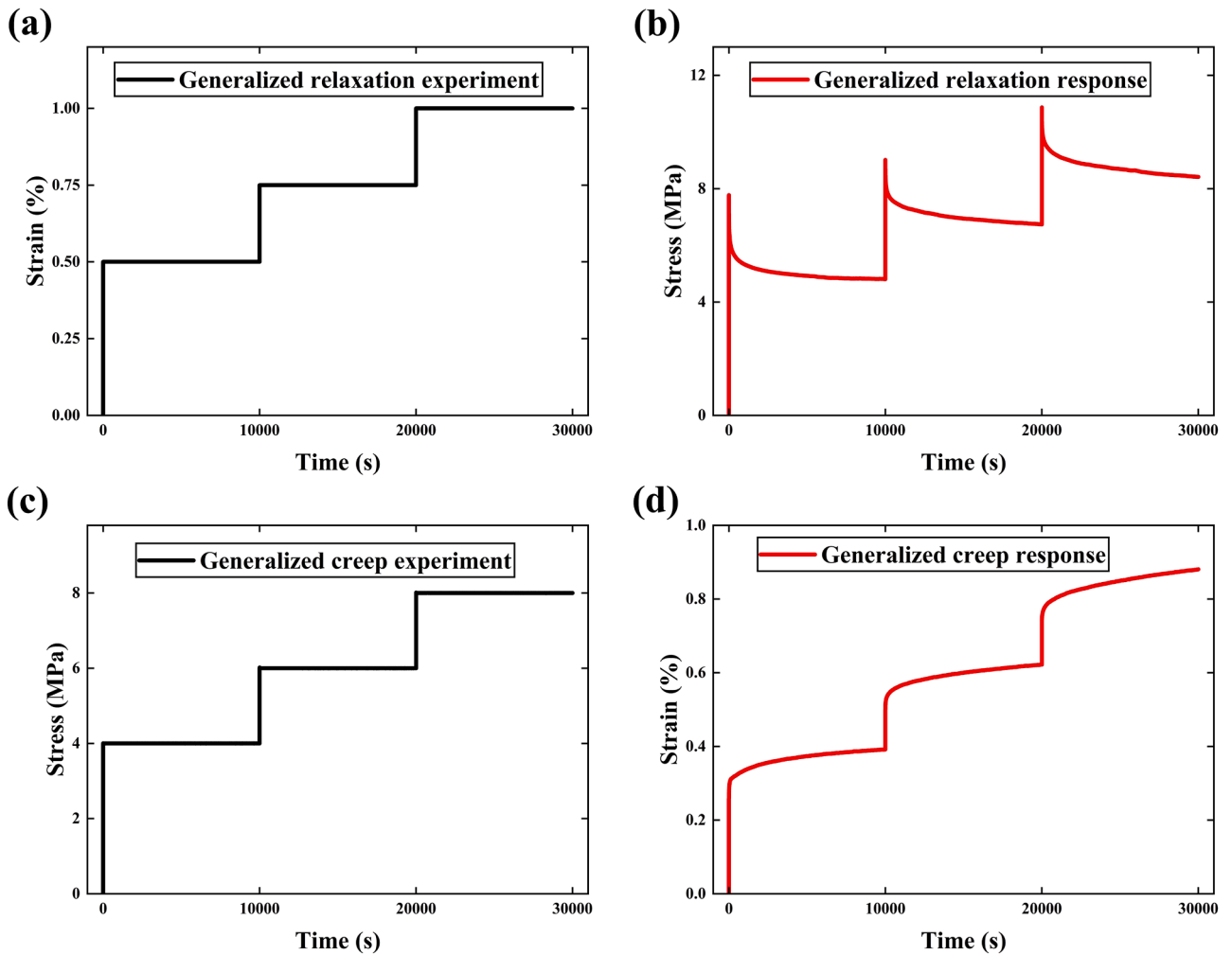


Fig. 6. Generalized relaxation and creep constitutive response of polypropylene. (a). Generalized relaxation experiment of polypropylene. (b). Generalized relaxation behavior response of polypropylene. (c). Generalized creep experiment of polypropylene. (d). Generalized creep behavior response of polypropylene.

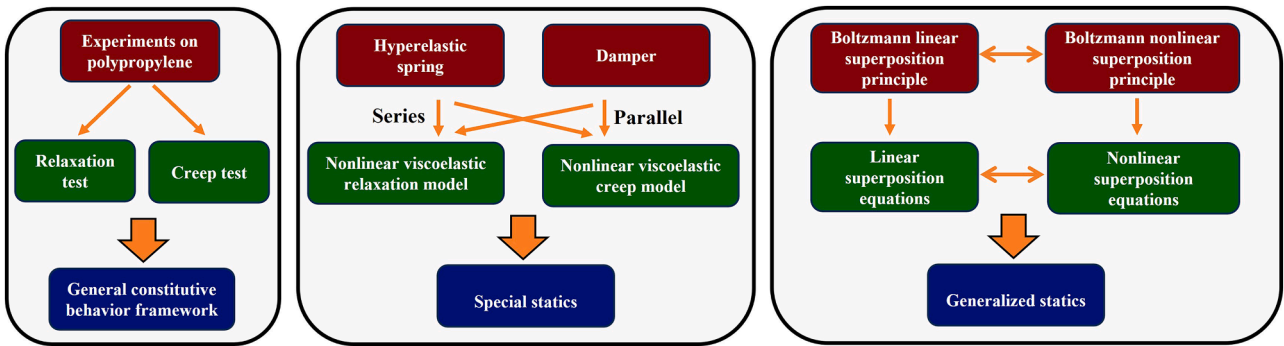


Fig. 7. The flowchart of the modeling method.

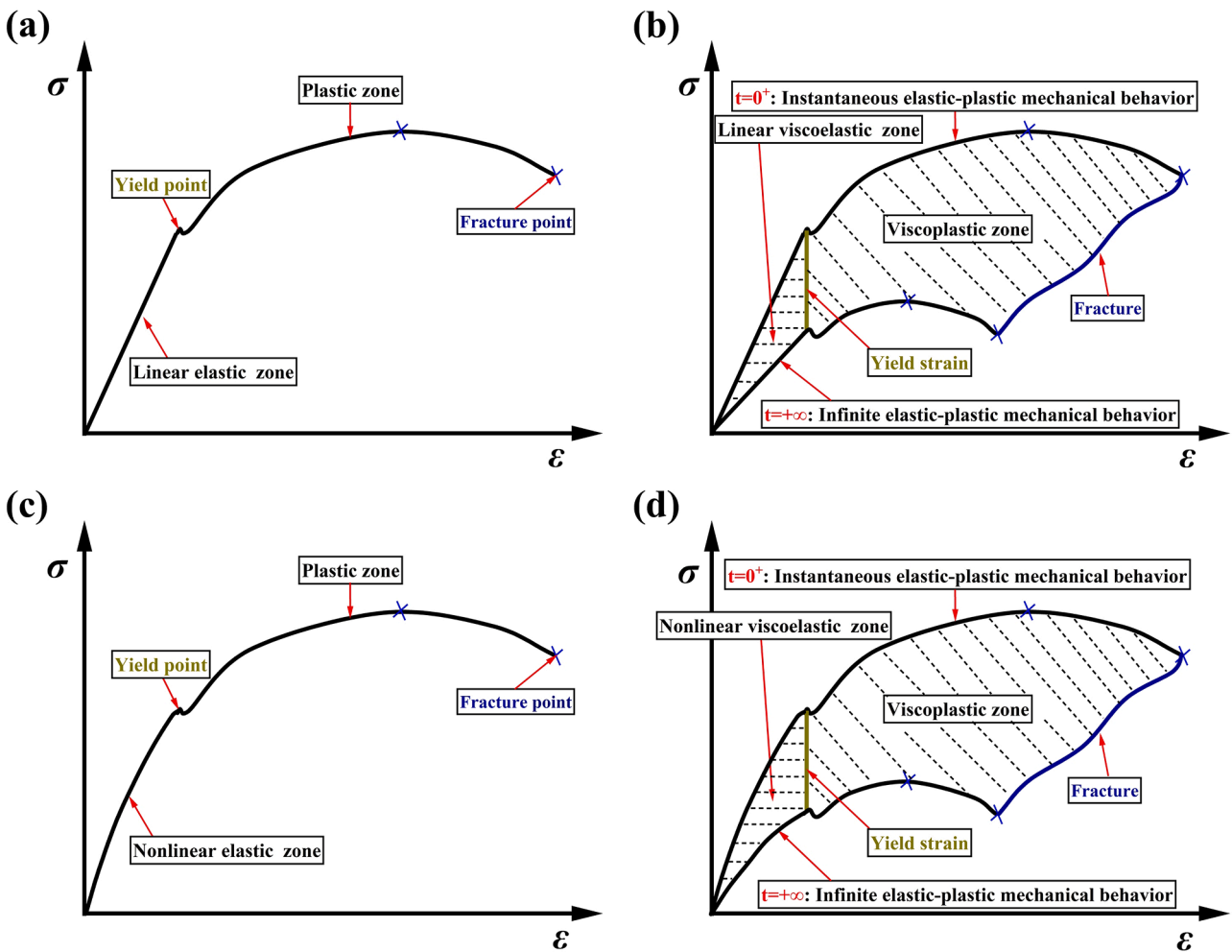


Fig. 8. General constitutive behavior framework of isotropic solid materials. (a). Linear elastic solids (Room-temperature metal materials). (b). Linear viscoelastic solids (High-temperature metal materials). (c). Nonlinear elastic solids or hyperelastic solids (Room-temperature rubber materials). (d). **The contribution of this work.** Nonlinear viscoelastic solids (Room-temperature polymer materials).

- Yield strain behavior
- Fracture behavior

Therefore, a general constitutive behavior framework for nonlinear viscoelastic solid materials is established (Fig. 8d).

4.2. Relaxation and creep constitutive behavior

The characteristic of linear viscoelastic stress relaxation and creep

behavior is the process of convergence from instantaneous linear elastic constitutive behavior (E_0) to infinite linear elastic constitutive behavior (E_∞) (Fig. 9a) [5]. However, for the relaxation and creep constitutive behavior of nonlinear viscoelastic solids, the characteristic is the process of convergence from instantaneous hyperelastic constitutive behavior (H_0) to infinite hyperelastic constitutive behavior (H_∞) (Fig. 9b).

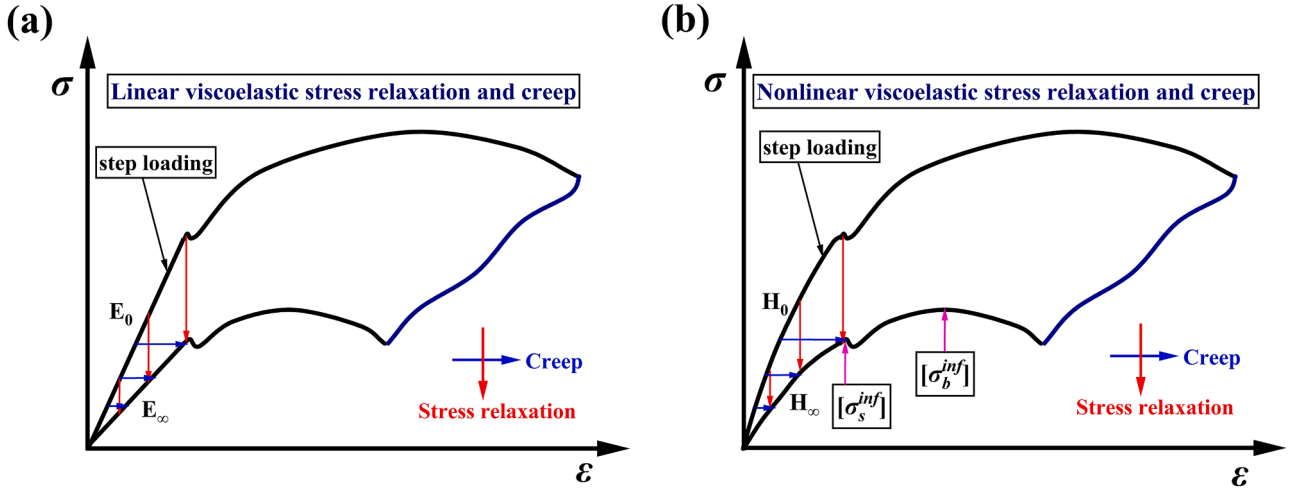


Fig. 9. Relaxation and creep constitutive behavior. (a). Linear viscoelastic stress relaxation and creep constitutive behavior. (b). **The contribution of this work.** Nonlinear viscoelastic stress relaxation and creep constitutive behavior. $[\sigma_s^{inf}]$ and $[\sigma_b^{inf}]$ are the yield and fracture strength of nonlinear viscoelastic solid materials.

4.3. Constitutive modeling

Considering that solid materials exhibit nonlinear damping behavior under dynamic loading conditions [40], while nonlinear damping behavior generally does not occur under static loading conditions. Modeling the nonlinear viscoelastic stress relaxation and creep consti-

ratio of incompressible materials is $\mu = 0.5$. The relation between the three principal strains is $\epsilon_{11} + \epsilon_{22} + \epsilon_{33} = 0$. The strain energy W is used to calculate the partial derivative of the strain tensor to obtain the stress tensor, which is written in the matrix form of the stress tensor and strain tensor as shown in Eq. (1b):

$$\begin{bmatrix} \sigma_{11} \\ \sigma_{22} \\ \sigma_{33} \\ \sigma_{23} \\ \sigma_{31} \\ \sigma_{12} \end{bmatrix} = \begin{bmatrix} C_{10} - C_{01} \cdot \epsilon_{11} & 0 & 0 & 0 & 0 & 0 \\ 0 & C_{10} - C_{01} \cdot \epsilon_{22} & 0 & 0 & 0 & 0 \\ 0 & 0 & C_{10} - C_{01} \cdot \epsilon_{33} & 0 & 0 & 0 \\ 0 & 0 & 0 & -2C_{01} & 0 & 0 \\ 0 & 0 & 0 & 0 & -2C_{01} & 0 \\ 0 & 0 & 0 & 0 & 0 & -2C_{01} \end{bmatrix} \begin{bmatrix} \epsilon_{11} \\ \epsilon_{22} \\ \epsilon_{33} \\ \epsilon_{23} \\ \epsilon_{31} \\ \epsilon_{12} \end{bmatrix}. \quad (1b)$$

tive behavior. The new constitutive model consists of a Newtonian fluid damper and a hyperelastic spring [24].

The constitutive model (Fig. 10) is a fundamental underlying logic in modeling, providing a closed convergent computational domain. Based on this underlying logic, many constitutive equations can be derived. In this article, the hyperelastic spring is characterized using an incompressible 2-parameter Mooney-Rivlin hyperelastic model. The strain energy function is shown in Eq. (1a) (Appendix A):

$$W = C_{10}(I_1 - 3) + C_{01}(I_2 - 3). \quad (1a)$$

Here, C_{10} and C_{01} are model parameters, with units of MPa. I_1 and I_2 are the first and second invariants of the strain tensor. The Poisson's

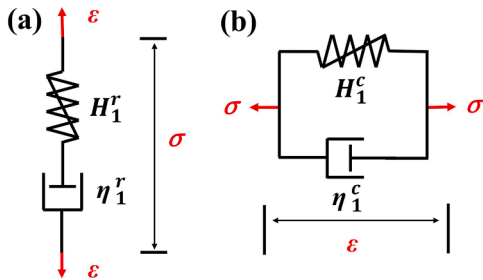


Fig. 10. Nonlinear viscoelastic models. (a). Maxwell-Mooney-Rivlin nonlinear viscoelastic fluid model. (b). Kelvin-Mooney-Rivlin nonlinear viscoelastic solid model.

Write it in tensor form:

$$\sigma_{ij}(\epsilon, t) = C_{ijkl} \cdot \epsilon_{kl}. \quad (1c)$$

Here, σ_{ij} , ϵ_{kl} are the stress tensor and strain tensor, respectively. C_{ijkl} hyperelastic matrix. Rewrite matrix Eq. (1b) as a stress tensor to represent the strain tensor, as shown in Eq. (1d):

$$\begin{bmatrix} \epsilon_{11} \\ \epsilon_{22} \\ \epsilon_{33} \\ \epsilon_{23} \\ \epsilon_{31} \\ \epsilon_{12} \end{bmatrix} = \begin{bmatrix} 0 & 0 & 0 \\ A_1 & 0 & 0 & 0 & 0 & 0 \\ 0 & A_2 & 0 & 0 & 0 & 0 \\ 0 & 0 & A_3 & 0 & 0 & 0 \\ 0 & 0 & 0 & \frac{1}{-2C_{01}} & 0 & 0 \\ 0 & 0 & 0 & 0 & \frac{1}{-2C_{01}} & 0 \\ 0 & 0 & 0 & 0 & 0 & \frac{1}{-2C_{01}} \end{bmatrix} \begin{bmatrix} \sigma_{11} \\ \sigma_{22} \\ \sigma_{33} \\ \sigma_{23} \\ \sigma_{31} \\ \sigma_{12} \end{bmatrix}. \quad (1d)$$

Here, $A_1 = \frac{C_{10} \pm \sqrt{C_{10}^2 - 4C_{01} \cdot \sigma_{11}}}{2C_{01} \cdot \sigma_{11}}$, $A_2 = \frac{C_{10} \pm \sqrt{C_{10}^2 - 4C_{01} \cdot \sigma_{22}}}{2C_{01} \cdot \sigma_{22}}$, $A_3 = \frac{C_{10} \pm \sqrt{C_{10}^2 - 4C_{01} \cdot \sigma_{33}}}{2C_{01} \cdot \sigma_{33}}$. Their dimension is MPa^{-1} , and Eq. (1d) is written in tensor Eq. (1e):

$$\epsilon_{ij}(\sigma, t) = D_{ijkl} \cdot \sigma_{kl}. \quad (1e)$$

The damper is characterized by Newton's law of viscosity. As shown in tensor Eq. (2):

$$\sigma_{ij} = \eta_{ijkl} \cdot \dot{\epsilon}_{kl} = \eta_{ijkl} \frac{d\epsilon_{kl}}{dt} \quad (2a)$$

Where η_{ijkl} is the viscosity coefficient, measured in MPa · s. Write in matrix form:

$$\begin{bmatrix} \sigma_{11} \\ \sigma_{22} \\ \sigma_{33} \\ \sigma_{23} \\ \sigma_{31} \\ \sigma_{12} \end{bmatrix} = \begin{bmatrix} \eta & 0 & 0 & 0 & 0 & 0 \\ 0 & \eta & 0 & 0 & 0 & 0 \\ 0 & 0 & \eta & 0 & 0 & 0 \\ 0 & 0 & 0 & \eta & 0 & 0 \\ 0 & 0 & 0 & 0 & \eta & 0 \\ 0 & 0 & 0 & 0 & 0 & \eta \end{bmatrix} \begin{bmatrix} \dot{\epsilon}_{11} \\ \dot{\epsilon}_{22} \\ \dot{\epsilon}_{33} \\ \dot{\epsilon}_{23} \\ \dot{\epsilon}_{31} \\ \dot{\epsilon}_{12} \end{bmatrix} \quad (2b)$$

Here, σ_{ij} , ϵ_{kl} , $\dot{\epsilon}_{kl}$ are the stress tensor, strain tensor, and strain rate tensor, respectively. η_{ijkl} is the viscosity matrix.

4.3.1. Nonlinear viscoelastic relaxation constitutive model

In 1867, Maxwell proposed the Maxwell linear viscoelastic fluid model, which consists of a linear elastic spring and a linear viscous damper connected in series. Considering the general nonlinear viscoelastic relaxation behavior characteristics (Fig. 9a), we propose the Maxwell-Mooney-Rivlin nonlinear viscoelastic fluid model, which consists of a hyperelastic spring (H_1^r) and a damper (η_1^r) connected in series (Fig. 10a). The constitutive equation derivation of Maxwell-Mooney-Rivlin fluid model is shown in Eq. (3):

$$\frac{d\epsilon_{kl}t}{dt} = \frac{1}{C_{ijkl}} \frac{\partial \sigma_{ij}(\epsilon, t)}{\partial t} + \frac{\sigma_{ij}(\epsilon, t)}{\eta_{ijkl}} \quad (3)$$

The new constitutive Eq. (4) is obtained by organizing the above equation:

$$\frac{\partial \sigma_{ij}(\epsilon, t)}{\partial t} + \frac{C_{ijkl}}{\eta_{ijkl}} \sigma_{ij}(\epsilon, t) = C_{ijkl} \frac{d\epsilon_{kl}t}{dt} \quad (4)$$

The Maxwell-Mooney-Rivlin model is subjected to a relaxation load of $\epsilon_{kl}t = \epsilon_{kl}\Delta(t)$, where ϵ_{kl} is constant strain and $\Delta(t)$ is the unit step function. The constitutive equation of the Maxwell-Mooney-Rivlin model is transformed into Eq. (5):

$$\frac{\partial \sigma_{ij}(\epsilon, t)}{\partial t} + \frac{C_{ijkl}}{\eta_{ijkl}} \sigma_{ij}(\epsilon, t) = 0 \quad (5)$$

Solving the tensor algebraic differential equation yields its specific solution, and the relaxation stress $\sigma_{ij}(\epsilon, t)$ of the Maxwell-Mooney-Rivlin nonlinear viscoelastic fluid model is Eq. (6):

$$\sigma_{ij}(\epsilon, t) = C_{ijkl} \cdot \epsilon_{kl} \cdot e^{-\frac{t}{\tau}} \quad (6)$$

The relaxation time τ is as shown in Eq. (7):

$$\tau = \frac{\eta_{ijkl}}{C_{ijkl}} \quad (7)$$

Six relaxation stress components are shown in Eq. (8a-b):

$$\begin{cases} \sigma_{ii}(\epsilon, t) = (C_{10} + C_{01} \cdot \epsilon_{ii}) \cdot \epsilon_{ii} \cdot e^{-\frac{t}{\tau_{ii}}}, \tau_{ii} = \frac{\eta}{C_{10} + C_{01} \cdot \epsilon_{ii}} \\ \sigma_{ij}(\epsilon, t) = -2C_{01} \cdot \epsilon_{ij} \cdot e^{-\frac{t}{\tau_{ij}}}, \tau_{ij} = \frac{\eta}{2C_{01}} \end{cases} \quad (8a-b)$$

Here, $\sigma_{ii}(\epsilon, t)$ represents three positive relaxation stresses, and $\sigma_{ij}(\epsilon, t)$ represents three shear relaxation stresses.

The generalized Maxwell-Mooney-Rivlin model (Fig. 11) consists of n Maxwell-Mooney-Rivlin nonlinear viscoelastic fluid models connected in parallel with infinite hyperelastic springs (H_∞). This can characterize the stress relaxation constitutive behavior of nonlinear viscoelastic solids (Fig. 9b). The Maxwell-Mooney-Rivlin nonlinear viscoelastic fluid model exhibits instantaneous Mooney-Rivlin hyperelastic behavior under step loading, and the hyperelastic spring stores elastic strain energy. Under constant strain, the damper (η_1^r) consumes the elastic strain energy (H_1^r) of the hyperelastic spring. Finally, the stress relaxation of the Maxwell-Mooney-Rivlin nonlinear viscoelastic fluid model reached 0 N. The stress of the generalized Maxwell-Mooney-Rivlin model converges to an infinite hyperelastic spring (H_∞) after infinite time.

For uniaxial tension, the relaxation stress of the generalized Maxwell-Mooney-Rivlin model is given by Eq. (9):

$$\sigma_{11}(\epsilon, t) = \sigma_{H_\infty}^{\epsilon_{11}} + \sum_1^n (C_{10}^i - C_{01}^i \cdot \epsilon_{11}) \cdot \epsilon_{11} \cdot e^{-\frac{t}{\tau_{11}^i}}, \tau_{11}^i = \frac{\eta_i}{(C_{10}^i - C_{01}^i \cdot \epsilon_{11})} \quad (9)$$

Here, $\sigma_{H_\infty}^{\epsilon_{11}}$ is the corresponding stress of Mooney-Rivlin infinite hyperelastic spring (H_∞) at a strain of ϵ_{11} . C_{10}^i and C_{01}^i are the model parameters of the Mooney-Rivlin hyperelastic spring in the i -th Maxwell-Mooney-Rivlin fluid model. η_i is the model parameter of the damper in the i -th Maxwell-Mooney-Rivlin fluid model. τ_{11}^i is the relaxation time of the damper in the i -th Maxwell-Mooney-Rivlin fluid model.

The relaxation modulus spectrum is shown in Eq. (10):

$$G_{11}(\epsilon, t) = \frac{\sigma_{H_\infty}^{\epsilon_{11}}}{\epsilon_{11}} + \sum_1^n (C_{10}^i - C_{01}^i \cdot \epsilon_{11}) \cdot e^{-\frac{t}{\tau_{11}^i}}, \tau_{11}^i = \frac{\eta_i}{(C_{10}^i - C_{01}^i \cdot \epsilon_{11})} \quad (10)$$

4.3.2. Nonlinear viscoelastic creep constitutive model

In 1875, Kelvin proposed the Kelvin linear viscoelastic solid model, which consists of a linear elastic spring and a damper connected in parallel. Considering the general nonlinear viscoelastic creep behavior characteristics (Fig. 9b), we propose the Kelvin-Mooney-Rivlin nonlinear viscoelastic solid model, which consists of a hyperelastic spring (H_1^r) and a damper (η_1^r) connected in parallel (Fig. 10b).

The derivation of the tensor algebraic calculus constitutive model for the Kelvin-Mooney-Rivlin solid model is as follows:

$$\sigma_{kl}(t) = \frac{\epsilon_{ij} \sigma, t}{D_{ijkl}} + \eta_{ijkl} \frac{d\epsilon_{ij} \sigma, t}{dt} \quad (11)$$

The Kelvin-Mooney-Rivlin solid model is subjected to a creep load of $\sigma_{kl}(t) = \sigma_{kl}\Delta(t)$, where σ_{kl} is the constant stress and $\Delta(t)$ is the unit step function. The creep strain $\epsilon_{ij} \sigma, t$ of the Kelvin-Mooney-Rivlin solid model can be obtained as follows:

$$\epsilon_{ij} \sigma, t = D_{ijkl} \cdot \sigma_{kl} \left(1 - e^{-\frac{t}{\lambda}} \right) \quad (12)$$

The creep retardation time λ is shown in Eq. (13):

$$\lambda = \eta_{ijkl} \cdot D_{ijkl} \quad (13)$$

Six creep strain components are shown in Eqs (14a-b):

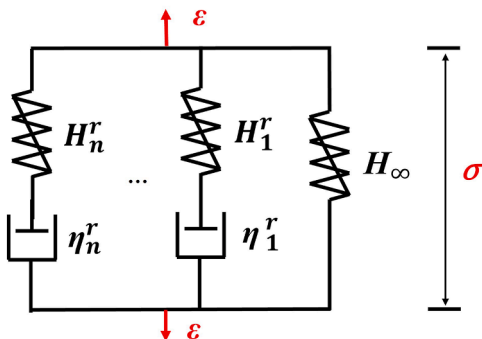


Fig. 11. Generalized Maxwell-Mooney-Rivlin constitutive model.

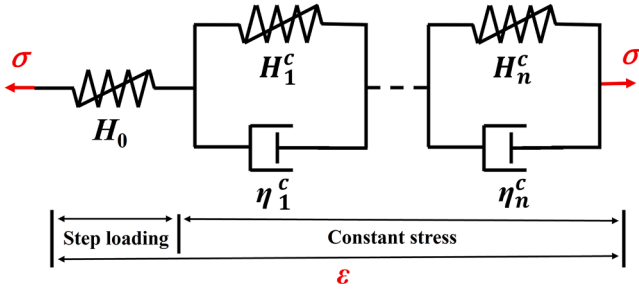


Fig. 12. Generalized Kelvin-Mooney-Rivlin constitutive model.

$$\begin{cases} \varepsilon_{ii}(\sigma, t) = A_1 \cdot \sigma_{ii} \cdot \left(1 - e^{-\frac{t}{\lambda_{ii}^c}}\right), \lambda_{ii} = \eta \cdot A_1. \\ \varepsilon_{ij}(\sigma, t) = \frac{\sigma_{ij}}{-2C_{01}^i} \cdot \left(1 - e^{-\frac{t}{\lambda_{ij}^c}}\right), \lambda_{ij} = -\frac{\eta}{2C_{01}^i}. \end{cases} \quad (14a-b)$$

Here, $\varepsilon_{ii}(\sigma, t)$ represents three positive creep strains, and $\varepsilon_{ij}(\sigma, t)$ represents three shear creep strains.

The generalized Kelvin-Mooney-Rivlin model (Fig. 12) consists of n Kelvin-Mooney-Rivlin nonlinear viscoelastic solid models connected in series with an instantaneous hyperelastic spring (H_0). This can characterize the creep constitutive behavior of nonlinear viscoelastic solids (Fig. 9b). The generalized Kelvin-Mooney-Rivlin model exhibits instantaneous Mooney-Rivlin hyperelastic behavior (H_0) under step loading. Under constant stress, the damper (η_1^c) delays the hyperelastic deformation (H_1^c) of the hyperelastic spring. Finally, the creep strain of the generalized Kelvin-Mooney-Rivlin model converges to the infinite hyperelastic behavior (H_∞).

In order to ensure the stability of the Mooney-Rivlin model, the parameters generally need to follow the rule of $C_{10}^i + C_{01}^i > 0$. For uniaxial tension, the creep strain of the generalized Kelvin-Mooney-Rivlin model is given by Eq. (15):

$$\varepsilon_{11}(\sigma, t) = \varepsilon_{H_\infty}^{\sigma_{11}} + \sum_1^n \frac{C_{10}^i - \sqrt{C_{10}^{i2} - 4C_{01}^i \cdot \sigma_{11}}}{2C_{01}^i \cdot \sigma_{11}} \cdot \sigma_{11} \cdot \left(1 - e^{-\frac{t}{\lambda_{11}^i}}\right). \quad (15)$$

Here, λ_{11}^i is the creep retardation time in the i -th Kelvin-Mooney-Rivlin model, as shown in Eq. (16):

$$\lambda_{11}^i = \eta_i \cdot \frac{C_{10}^i - \sqrt{C_{10}^{i2} - 4C_{01}^i \cdot \sigma_{11}}}{2C_{01}^i \cdot \sigma_{11}}. \quad (16)$$

$\varepsilon_{H_\infty}^{\sigma_{11}}$ is the strain corresponding to the instantaneous hyperelastic spring (H_0) at a stress of σ_{11} . C_{10}^i and C_{01}^i are the model parameters of the Mooney-Rivlin hyperelastic spring in the i -th Kelvin-Mooney-Rivlin solid model. η_i is the model parameter of the damper in the i -th Kelvin-Mooney-Rivlin solid model.

The creep compliance spectrum is shown in Eq. (17):

$$J_{11}(\sigma, t) = \frac{\varepsilon_{H_\infty}^{\sigma_{11}}}{\sigma_{11}} + \sum_1^n \frac{C_{10}^i - \sqrt{C_{10}^{i2} - 4C_{01}^i \cdot \sigma_{11}}}{2C_{01}^i \cdot \sigma_{11}} \cdot \left(1 - e^{-\frac{t}{\lambda_{11}^i}}\right). \quad (17)$$

4.4. Boltzmann superposition principle and Boltzmann's equations

The Boltzmann superposition principle provides a qualitative mechanistic description of single-physics field superposition in solid materials. The corresponding Boltzmann's equations represents its quantitative mathematical formulation.

4.4.1. Boltzmann superposition principle

In 1874, Boltzmann established the Boltzmann linear superposition principle [3,4]. It describes the strain and stress response of linear solid materials under generalized relaxation and creep loads. However, there is still no unified analytical equation linking special statics and generalized statics for nonlinear solid materials (Fig. 1). The Boltzmann superposition principle is the core concept of linear viscoelastic constitutive theory and is not applicable to describing the mechanical behavior of nonlinear viscoelasticity. Therefore, Zhou et al. [24] proposed a method based on the physical concept of 'anchored', which can be qualitatively transformed from linear to nonlinear. The detailed process is shown below:

- (1) The contribution of micro stress/micro strain applied in each stage to the final total deformation/relaxation remains independent, and the final total deformation/relaxation is the superposition of deformation/relaxation caused by micro stress/micro strain in each stage.
- (2) Linear materials (linear elastic solids, linear viscoelastic solids) follow a linear superposition constitutive relation. The contribution of micro stress/micro strain is the same; The total deformation/total relaxation is a linear superposition of the contributions of micro stress/micro strain in each stage (Fig. 13a).
- (3) Nonlinear materials (nonlinear elastic solids, nonlinear viscoelastic solids) follow a nonlinear superposition constitutive relation. The deformation/relaxation contributions caused by micro stress/micro strain are different, and the total deformation/total relaxation is a nonlinear superposition of micro stress/micro strain contributions in each stage (Fig. 13b).

The Boltzmann superposition principle qualitatively unifies the constitutive relation of single physics field superposition in solid mechanics.

4.4.2. Boltzmann's equations

The strain of a linear viscoelastic material at any given moment depends on everything that has happened before, that is, the entire stress history $\sigma(\tau)$ that depends on $\tau < t$. The creep compliance $J(t)$ in the linear superposition principle followed by linear viscoelastic materials is stress-independent. The strain of nonlinear viscoelastic solid materials at any given time also depends on everything that has occurred previously, that is, on the entire stress history $\sigma(\tau)$ of $\tau < t$. This effect is called long-tail memory effect [41]. Unlike linear viscoelastic materials, nonlinear viscoelastic materials follow a nonlinear superposition principle in which the creep compliance spectrum $J(\sigma, t)$ is stress-dependent. The Boltzmann's equations are the mathematical form of the Boltzmann superposition principle. The derivation of its nonlinear superposition constitutive relation is as follows:

$$\varepsilon(\sigma, t) = \sigma(\tau) \cdot J[\sigma(\tau), t]. \quad (18)$$

Here,

$$\varepsilon(\sigma, t) = \varepsilon_1(t) + \varepsilon_2(t) + \dots + \varepsilon_n(t) = \sum_{i=1}^n \Delta\sigma_i(\tau) \cdot J[\sigma_i(\tau), t - \tau]. \quad (19)$$

Here,

$$\Delta\sigma(\tau) = \sigma(\tau + d\tau) - \sigma(\tau) \approx d\sigma = \frac{d\sigma(\tau)}{d\tau} \cdot d\tau. \quad (20)$$

Here, the creep strain contributed by $d\sigma$ is

$$d\varepsilon(\sigma, t) = d\sigma \cdot J[\sigma_i(\tau), t - \tau] = J[\sigma_i(\tau), t - \tau] \frac{d\sigma(\tau)}{d\tau} \cdot d\tau. \quad (21)$$

Continuing Eq. (21) yields Eq. (22):

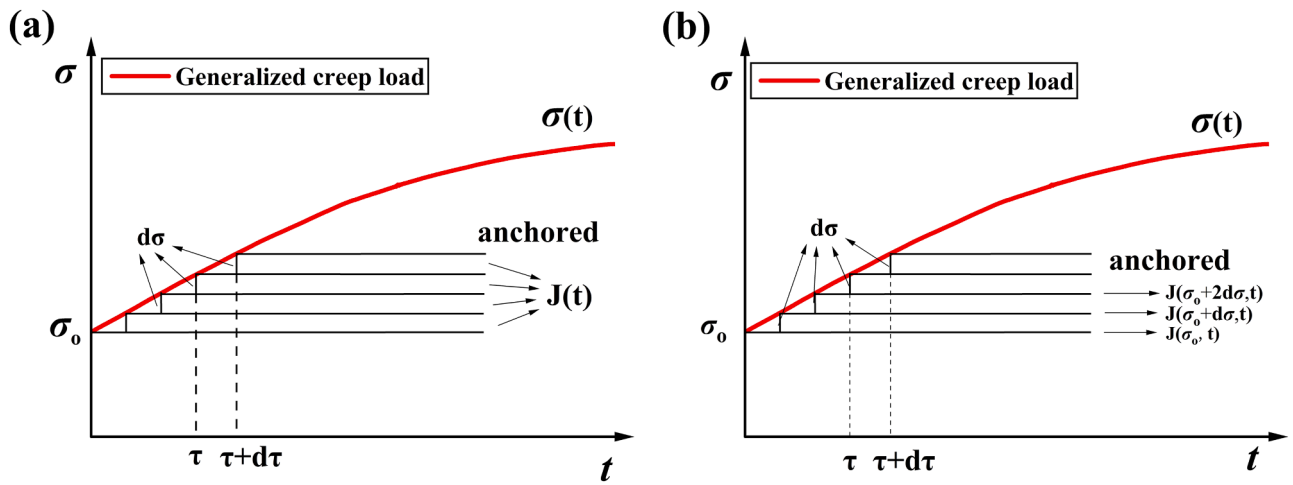


Fig. 13. Boltzmann superposition principle. (a). Linear viscoelastic material: Principle of linear superposition. (b). Nonlinear viscoelastic materials: Principle of nonlinear superposition.

$$\epsilon(\sigma, t) = \int_0^t J[\sigma(\tau), t - \tau] \frac{d\sigma(\tau)}{d\tau} d\tau. \quad (22)$$

On the contrary, the bridge equation between the special and generalized stress relaxation behaviors of nonlinear viscoelastic solids can be obtained, as shown in Eq. (23):

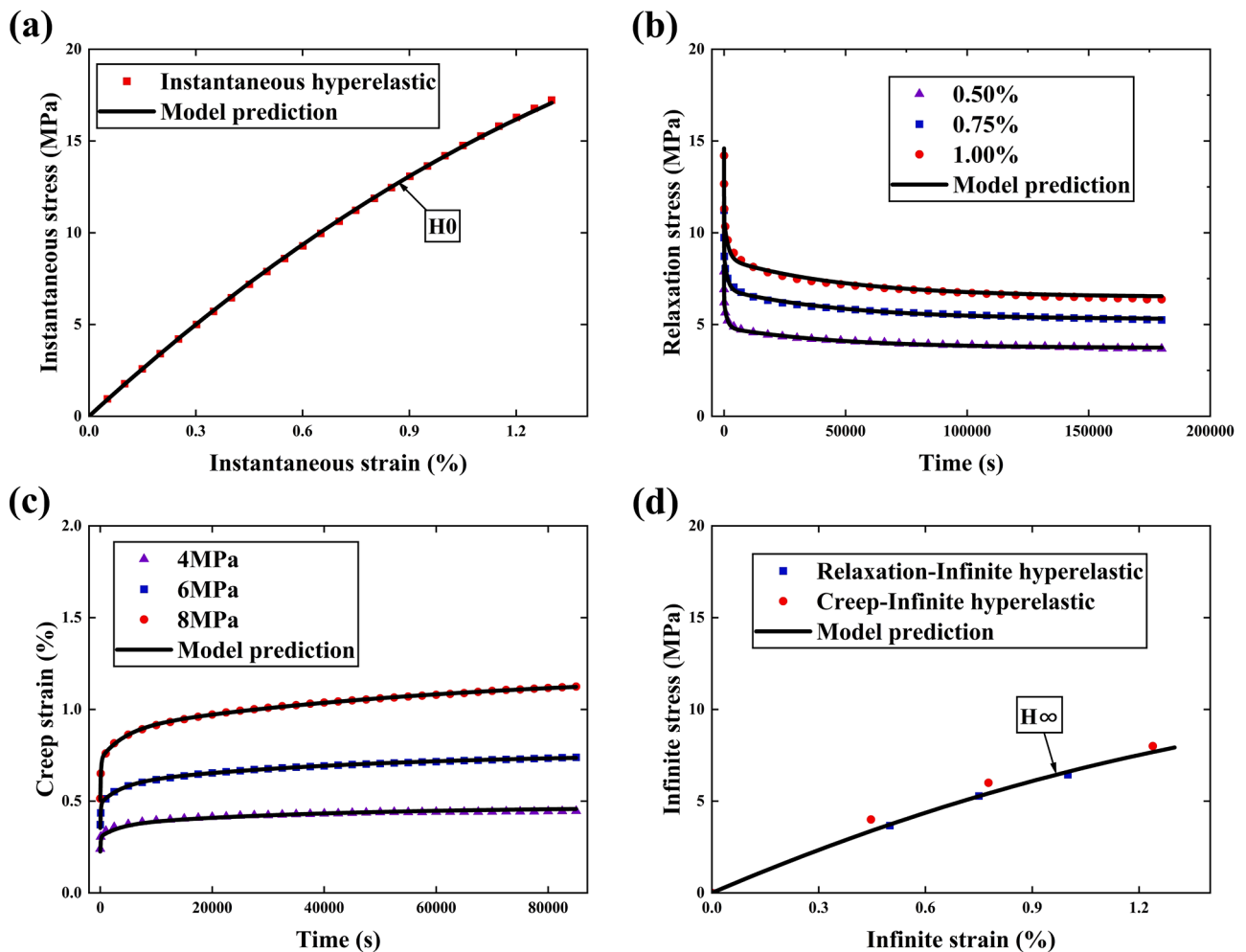


Fig. 14. Nonlinear viscoelastic constitutive behavior and model prediction. (a). Instantaneous hyperelastic constitutive behavior and instantaneous Mooney-Rivlin model prediction. (H_0). (b). Nonlinear stress relaxation constitutive behavior and generalized Maxwell-Mooney-Rivlin model prediction. (c). Nonlinear creep constitutive behavior and generalized Kelvin-Mooney-Rivlin model prediction. (d). Infinite hyperelastic constitutive behavior and Infinite Mooney-Rivlin model prediction (H_∞).

$$\sigma \varepsilon, t = \int_0^t G[\varepsilon(\tau), t - \tau] \frac{d\varepsilon(\tau)}{d\tau} d\tau. \quad (23)$$

Combining the two linear superposition constitutive equations described by Boltzmann [3,4], we have established the Boltzmann's equations, as shown in Eqs (24a-d):

$$\left\{ \begin{array}{l} \varepsilon t = \sigma_0 \cdot J(t) + \int_0^t J(t - \tau) \frac{d\sigma(\tau)}{d\tau} d\tau. \\ \sigma t = \varepsilon_0 \cdot G(t) + \int_0^t G(t - \tau) \frac{d\varepsilon(\tau)}{d\tau} d\tau. \\ \varepsilon(\sigma, t) = \sigma_0 \cdot J(\sigma_0, t) + \int_0^t J[\sigma(\tau), t - \tau] \frac{d\sigma(\tau)}{d\tau} d\tau. \\ \sigma \varepsilon, t = \varepsilon_0 \cdot G(\varepsilon_0, t) + \int_0^t G[\varepsilon(\tau), t - \tau] \frac{d\varepsilon(\tau)}{d\tau} d\tau. \end{array} \right. \quad (24a-d)$$

The Boltzmann's equations provide a complete and unified summary of the basic laws of solid materials under static loads, pushing the single physical field superposition constitutive relation of solid mechanics to a new height. It is a bridge equation system that links special statics (Fig. 1a) and generalized statics (Fig. 1b).

5. Comparison between experimental and theoretical results

Section 5 presents systematic comparisons between experimental measurements and theoretical predictions. First, model predictions for nonlinear viscoelastic relaxation and creep behavior are validated against experimental PP data. Subsequently, the predictive capability of the Boltzmann equation is extended to characterize generalized relaxation and creep behavior under multi-stage loading conditions.

5.1. Prediction of nonlinear viscoelastic models

The experimental data verification of the incompressible nonlinear viscoelastic stress relaxation and creep constitutive model constructed under uniaxial tension of PP. Use the Mooney-Rivlin model (Eq. 1a) in the ABAQUS finite element software material model library to predict the instantaneous hyperelastic constitutive behavior of PP. Fig. 14a compares the experimental results with the model, which fully describes the instantaneous hyperelastic constitutive behavior of PP. The nonlinear viscoelastic stress relaxation constitutive equation (Eq. 9) was used to predict the stress relaxation constitutive behavior of PP. Using the Origin software for fitting, Fig. 14b shows the generalized Maxwell-Mooney-Rivlin model capturing the nonlinear relaxation behavior under three different constant strains (0.5 %, 0.75 %, and 1 %). The parameters of the nonlinear relaxation model are shown in Table 1. Based on the nonlinear viscoelastic stress relaxation model and model parameters, the relaxation behavior covering the entire nonlinear viscoelastic zone can be predicted, with constant strain ranging from 0 to 1.3 %.

The nonlinear creep constitutive behavior of PP was predicted using the nonlinear viscoelastic creep constitutive equation (Eq. 15). Using the Origin software for fitting, Fig. 14c shows the generalized Kelvin-

Mooney-Rivlin model capturing the nonlinear creep behavior under three different constant stresses (4, 6, and 8 MPa). The parameters of the nonlinear creep model are shown in Table 2. Based on the nonlinear viscoelastic creep model and model parameters, the creep behavior covering the entire nonlinear viscoelastic zone can be predicted, with constant stress ranging from 0 to 8 MPa. Three sets of relaxation and three sets of creep experimental data converge to an infinite hyperelastic behavior after infinite time (Fig. 14d). Use the Mooney-Rivlin model (Eq. 1a) in the ABAQUS finite element software material model library to predict the infinite hyperelastic constitutive behavior of PP (Fig. 14d). The models constructed in this study effectively predicted the experimental results of PP under uniaxial tension, with an overall prediction accuracy ($R^2 > 0.98$).

5.2. Prediction of Boltzmann's equations

The nonlinear generalized relaxation and creep constitutive behavior of PP was predicted using the Boltzmann nonlinear superposition principle and Boltzmann's equations (Eqs. 24c-d). Overall, the subsequent evolution of the generalized relaxation stage in the first, second, and third stages matches the experimental data well with the non-linear viscoelastic superposition. (Fig. 15a). The nonlinear viscoelastic superposition of generalized creep constitutive behavior was well captured by the model prediction for the first, second, and third nonlinear viscoelastic superposition constitutive behaviors (Fig. 15b).

6. Discussion

Section 6 is structured into three components: General constitutive behavior framework, Methodology for nonlinear viscoelastic constitutive modeling, and Boltzmann superposition principle and Boltzmann's equations.

6.1. General constitutive behavior framework

Determining the stability of viscoelastic structures remains a challenging task. Seemingly stable conformations of viscoelastic structures may gradually creep until their stability is lost, while a discernible creeping in viscoelastic solids does not necessarily lead to instability [42]. The issue of structural stability is to determine the threshold stress between low-stress creep stability and high-stress creep instability, and the threshold stress must be obtained through experiments. For example, Huo et al. [43] proposed a new constitutive relationship for high-temperature creep of alloys. Among them, At 550 °C, constant low-stress (835 and 850 MPa) maintains creep stability, while constant high-stress (890 and 920 MPa) leads to creep instability and creep fracture. However, the creep stability of alloys is uncertain when the creep stress is around 850~890 MPa. At 600 °C, constant low-stress (730 MPa) maintains creep stability, while constant high-stress (780 and 815 MPa) leads to creep instability and creep fracture. However, the creep stability of alloys is uncertain when the creep stress is around 730~780 MPa. The essence of the long-standing problem that has plagued people is the lack of a theoretical framework to predict the future stability of these systems [42-44]. Zhou et al. [5] established a general constitutive behavior framework for metal alloys at any constant high temperature, defining the yield strength and fracture strength of metals at any

Table 1
Generalized Maxwell-Mooney-Rivlin model parameters.

H_∞	C_{01}^∞ (MPa)	η_1^r	H_1^r	C_{01}^1 (MPa)	η_2^r
C_{10}^∞ (MPa)	C_{01}^∞ (MPa)	η_1 (MPa · s)	C_{10}^1 (MPa)	C_{01}^1 (MPa)	η_2 (MPa · s)
-2659.235	2798.023	4897.802	411.2609	2553.5468	355300.869
H_2^r	C_{01}^2 (MPa)	η_3^r	H_3^r	C_{01}^3 (MPa)	
C_{10}^2 (MPa)	C_{01}^2 (MPa)	η_3 (MPa · s)	C_{10}^3 (MPa)	C_{01}^3 (MPa)	
338.19191	12292.9652	10335995.7	237.57643	2809.3013	

Table 2
Generalized Kelvin-Mooney-Rivlin model parameters.

H_0		η_1^c	H_1^f	η_2^c	
C_{10}^0 (MPa)	C_{01}^0 (MPa)	η_1 (MPa · s)	C_{10}^1 (MPa)	C_{01}^1 (MPa)	η_2 (MPa · s)
-5486.1665	5782.14912	4794.8691	58.306613	99.882724	214285.009
H_2		η_3^c	H_5^f		
C_{10}^2 (MPa)	C_{01}^2 (MPa)	η_3 (MPa · s)	C_{10}^3 (MPa)	C_{01}^3 (MPa)	
69.245737	119.9964	1604604.37	47.463378	70.247691	

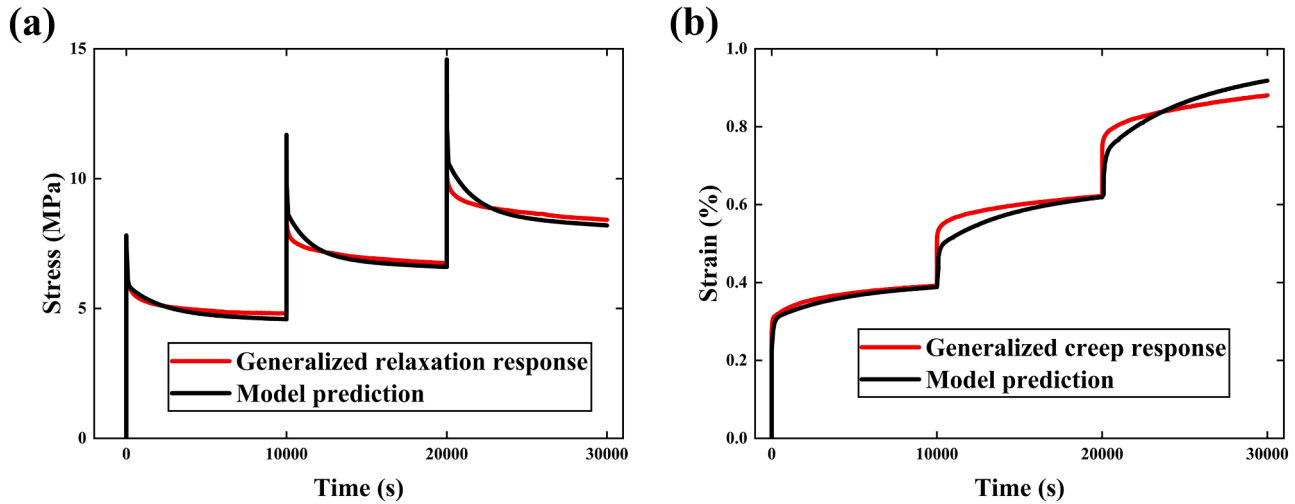


Fig. 15. Boltzmann nonlinear superposition constitutive relation and model prediction. (a). Comparison between generalized relaxation constitutive behavior and Boltzmann's equations. (b). Comparison between generalized creep constitutive behavior and Boltzmann's equations.

constant high temperature (Fig. 8b & 9a). This improvement resolved creep stability prediction for metals across all high temperatures. By analogy, it is imperative to establish a general constitutive behavior framework for nonlinear viscoelastic solid materials.

The key to our analysis of stability in nonlinear viscoelastic materials lies in the discovery of a new stationarity property. Previously, numerous researchers have investigated the stress relaxation and creep properties of nonlinear viscoelastic solid materials from an experimental perspective. This encompasses biomaterials like cartilage [17], trabecular bone [18], intervertebral disc [45], biological tissues [46] and bovine cortical bone [47]. It also includes non-biomaterials such as PP [19,36], Poly-Ether-Ether-Ketone [48], polyurethane rubber [49], asphalt [50] and salt rock [51], among others.

Unlike in previous experiments, we have established a general constitutive behavior framework (Fig. 8d) for nonlinear viscoelastic solid materials on the basis of the experimental results. This framework has the ability to predict future creep stability. The infinite hyperelastic-plastic constitutive behavior is the only static stable boundary. This is a process of convergence from an instantaneous hyperelastic-plastic boundary to an infinite hyperelastic-plastic boundary. Any static constitutive behavior either converges to an infinite hyperelastic-plastic static stable boundary or does not converge but tends towards fracture. This was experimentally verified by stress relaxation (Fig. 3) and creep (Fig. 4). Our contribution is to solve the threshold stress problem of creep stability in nonlinear viscoelastic solids. The threshold stress is defined as the yield strength and fracture strength. This is a goal that previous researchers have not achieved [42,43,52]. In this study, the yield strength of PP is 8 MPa and the fracture strength is 13 MPa. The general constitutive behavior framework represents an improvement from qualitative to quantitative analysis for the creep stability analysis of nonlinear viscoelastic solids (Fig. 8d & 9b).

6.2. Methodology for nonlinear viscoelastic constitutive modeling

In the classical linear viscoelastic constitutive theory, the relaxation modulus $G(t)$ of the generalized Maxwell model and the creep compliance $J(t)$ of the generalized Kelvin model are shown in Eqs (25) and (26) [53–56]. It is also known as the Prony series [57].

$$G(t) = E_\infty + \sum_{i=1}^n E_i e^{-\frac{t}{\tau_i}} \tag{25}$$

$$J(t) = \frac{1}{E_0} + \sum_{i=1}^n \frac{1}{E_i} \left(1 - e^{-\frac{t}{\tau_i}} \right) \tag{26}$$

The relaxation modulus $G(t)$ and creep compliance $J(t)$ can be spatially transformed into the relaxation modulus spectrum $G(\epsilon, t)$ and creep compliance spectrum $J(\sigma, t)$ [24]. Thus, $G(t) = G(\epsilon, t)$, $J(t) = J(\sigma, t)$. Based on the general constitutive behavior framework (Fig. 8d). The nonlinear viscoelastic behavior indicates the characteristic of convergence from an instantaneous hyperelastic boundary to an infinite hyperelastic boundary due to the time-independent energy stored in the elastic part and the time-dependent energy lost in the viscous part (Fig. 9b). The nonlinear viscoelastic relaxation modulus spectrum $G(\epsilon, t)$ and creep compliance spectrum $J(\sigma, t)$ are strain dependent and stress dependent, respectively. Therefore, linear viscoelasticity (Fig. 9a) is the limit or special case of nonlinear viscoelasticity (Fig. 9b).

To the best of our knowledge, this study is the first manuscript modeled based on a general constitutive behavior framework (Fig. 8d & 9b). Among them, the boundary of instantaneous hyperelastic and infinite hyperelastic behavior (Fig. 9b) is also the boundary of the constitutive model (Fig. 11 & 12). This modeling feature draws on and extends the generalized Maxwell and Kelvin linear viscoelastic theories. Replace the Mooney-Rivlin spring in the generalized Maxwell-Mooney-Rivlin model with a linear elastic spring, and transform the model into

the generalized Maxwell model. The nonlinear viscoelastic stress relaxation model Eq. (10) is transformed into a linear viscoelastic stress relaxation Eq. (25). Among them, the parameters C_{10} and C_{01} of the Mooney-Rivlin model replace the Young's modulus in linear viscoelastic theory. The nonlinear viscoelastic relaxation modulus spectrum is transformed into a linear viscoelastic relaxation modulus. Replace the Mooney-Rivlin spring in the generalized Kelvin-Mooney-Rivlin model with a linear elastic spring, and transform the model into a generalized Kelvin model. The nonlinear viscoelastic creep model Eq. (17) is transformed into a linear viscoelastic creep Eq. (26). Among them, the parameters C_{10} and C_{01} of the Mooney-Rivlin model replace the Young's modulus in linear viscoelastic theory. The nonlinear viscoelastic creep compliance spectrum is transformed into a linear viscoelastic creep compliance.

The development of nonlinear viscoelastic solid constitutive models dates back to early studies, with foundational approaches relying on superpositions of hyperelastic and viscoelastic components [58,59]. For instance, this strategy has been applied to model hydrogels [60,61]. However, our novel approach integrates a hyperelastic model with Newtonian viscous mechanics. While instantaneous hyperelasticity aligns with prior work, the hyperelastic component is embedded within the overall nonlinear viscoelastic framework, abolishing the independence between hyperelasticity and viscoelasticity. A unique aspect of this model is the definition of infinite hyperelastic limits, which extends temporal characterization to infinite time—a feature absent in previous formulations. These innovations distinguish our nonlinear viscoelastic modeling approach from existing hydrogel models [60,61].

The primary innovation of this study lies in the development of a methodology for constructing nonlinear viscoelastic constitutive relations. For the first time, we propose a "underlying architecture" based on series-parallel configurations of hyperelastic springs and dampers (Fig. 10). It is the most fundamental and core structural design in the future nonlinear viscoelastic theory system, which determines the operational logic, scalability, and stability of the entire system.

The construction of the hyperelastic constitutive theory system mainly focused on the 20th century. Table 3 presents the strain energy functions (W) of several major classical incompressible hyperelastic theoretical models. Based on our proposed "underlying architecture" logic. Building upon this foundational architecture, constructing Maxwell-Mooney-Rivlin, Maxwell-Yeoh, Maxwell-Blatz-Ko, and Maxwell-Ogden nonlinear viscoelastic relaxation fluid models proves relatively straightforward. However, the most difficult point in constructing nonlinear viscoelastic creep models is that they may not be able to be expressed using explicit equations.

To derive the explicit form of the Kelvin-Mooney-Rivlin creep model, the strain tensor invariants were reduced to principal strain tensor invariants, enabling the Mooney-Rivlin model to be represented as a diagonal matrix (Appendix A). This transformation facilitates explicit expression of the nonlinear creep equation. Notably, the constitutive equation developed in this study is restricted to uniaxial/biaxial tensile loadings of nonlinear viscoelastic solid materials. Its inability to be directly integrated with finite element methods for complex stress conditions represents a limitation to be addressed in future research.

Regarding model generalizability, we observed that increasing the number of Maxwell-Mooney-Rivlin fluid and Kelvin-Mooney-Rivlin

solid units improves fitting accuracy during parameter identification. Ultimately, three units were selected for each model to characterize PP behavior. Secondly, it is essential to emphasize that nonlinear viscoelastic behavior represents a convergence process from instantaneous hyperelasticity (the initial state of relaxation/creep) to infinite hyperelasticity (the terminal state of relaxation/creep). The instantaneous hyperelasticity curve serves as the starting point for relaxation and creep responses, while the infinite hyperelasticity curve represents their long-term convergence limit. Accurate characterization of these two hyperelastic states is critical for modeling nonlinear relaxation and creep behavior. Notably, hyperelastic models such as Mooney-Rivlin exhibit superior fitting precision for highly nonlinear elastic behaviors with inflection points. Therefore, when generalizing this framework to other polymeric materials, maintaining boundary accuracy between instantaneous and infinite hyperelasticity is pivotal for ensuring predictive reliability.

Early hyperelastic constitutive models were only applicable to incompressible solids such as rubber. The Poisson's ratio of rubber is 0.49. Flory et al. [62] (Nobel Prize winner in Chemistry) first suggested dividing local deformation into "volumetric part" and "isocholic part", with the former corresponding to volume changes and the latter corresponding to shear deformation. The compressible Mooney-Rivlin hyperelastic constitutive model is shown in Eq. (27) [63,64]:

$$W = C_{10}(I_1 - 3) + C_{01}(I_2 - 3) + \frac{1}{D_1}(J - 1)^2. \quad (27)$$

Here, D_1 is a parameter related to the compressibility of the material. Accordingly, compressible solid models are constructed by adding compressible terms to incompressible frameworks. However, this study only derived the nonlinear viscoelastic relaxation and creep characteristics of incompressible isotropic solids. On the one hand, the Poisson's ratio of PP is 0.42, rather than the theoretically incompressible 0.5. The assumption of incompressibility limits the applicability of the model to micro compressible solid materials (Poisson's ratio 0.45-0.5). However, incompressible models are the foundation for establishing compressible models in the future.

On the other hand, the Mooney-Rivlin model was originally developed to describe large deformation (>5 %) engineering applications of rubber materials, such as tires and sealing elements. Rubber can undergo strains up to 500 %, requiring stress-strain measurements based on the second Piola-Kirchhoff stress tensor and right Cauchy-Green strain tensor. The first, second, and third invariants of the strain tensor are the eigenvalues of the right Cauchy-Green strain tensor [63,65]. In contrast, nonlinear viscoelastic deformations of polymers typically involve small strains (<5 %). PP viscoelastic strain in this study remained below 1.3 % (Fig. 4f). Under the small deformation assumption, strain tensor invariants in this work are defined using eigenvalues of the Cauchy strain tensor (Appendix A). Notably, many biomaterials—e.g., enamel and trabecular bone—exhibit small deformations, while others like cartilage, muscle, and blood vessels can sustain 50–100 % strains. Biomaterial applications thus depend crucially on appropriate strain tensor measurements. Future studies will focus on developing constitutive models for compressible solids under large deformations, while this work restricts itself to incompressible solids and small deformations.

6.3. Boltzmann superposition principle and Boltzmann's equations

The relaxation modulus $G(t)$ in the Maxwell model and the creep compliance $J(t)$ in the Kelvin model can be substituted into the Boltzmann linear superposition equations (Fig. 16). It can characterize the constitutive behavior of linear viscoelastic solid materials under generalized relaxation and creep loads. As a cornerstone of classical viscoelasticity, the Boltzmann linear superposition principle [3,4], bridges special statics (Fig. 1a) and generalized statics (Fig. 1b).

For nonlinear viscoelastic solid materials, the linear superposition principle fails to apply. Green and Rivlin [29] proposed an approximate

Table 3
Several classic hyperelastic constitutive strain energy functions.

Constitutive models	Strain energy functions (W)
Neo-Hookean	$C_{10}(I_1 - 3)$
Mooney-Rivlin	$C_{10}(I_1 - 3) + C_{01}(I_2 - 3)$
Yeoh	$C_{10}(I_1 - 3) + C_{20}(I_1 - 3)^2 + C_{30}(I_1 - 3)^3$
Blatz-Ko	$\frac{\mu}{2} \left(\frac{I_2}{I_3} + 2\sqrt{I_3} \right)$
Ogden	$\sum_{i=1}^N \frac{\mu_i}{\alpha_i} (\lambda_1^{\alpha_i} + \lambda_2^{\alpha_i} + \lambda_3^{\alpha_i} - 3)$

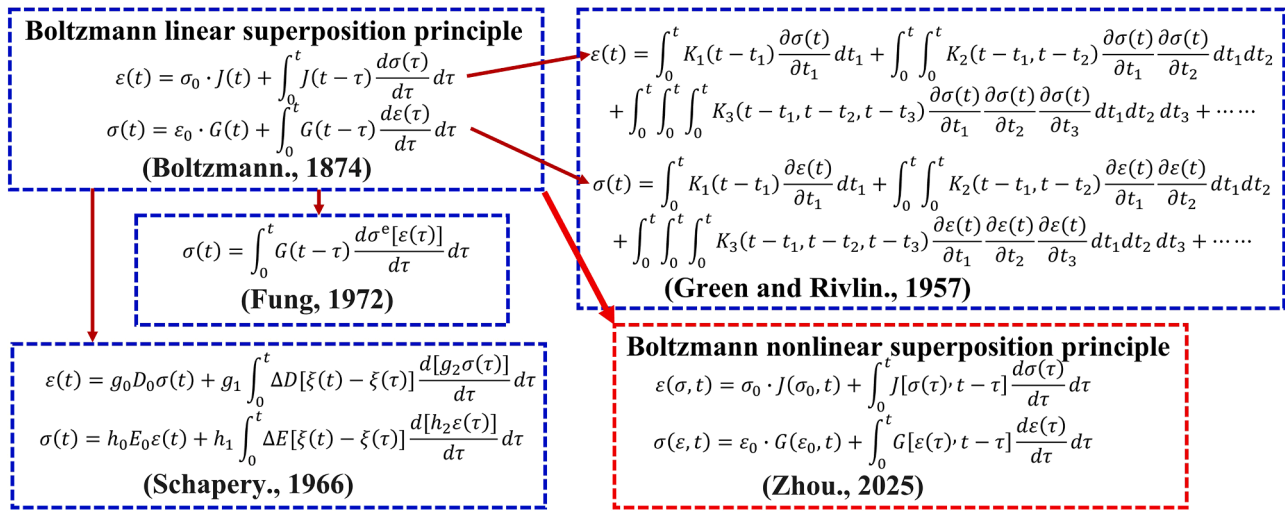


Fig. 16. The development history of single physics field superposition in solid materials.

equations (Fig. 16) for linking the special statics (Fig. 1a) and generalized statics (Fig. 1b) of nonlinear solids. However, they are not analytical equations. Building upon the first three terms of their approximation, power-law formulations have been developed to characterize nonlinear creep behavior, such as Eq. (28) [33–35]. Nutting’s law [66,67], a widely adopted creep model, adopts a power-law form expressed as: $\varepsilon(\sigma, t) = \varepsilon_0 + A\sigma^n t^n$.

$$\varepsilon(\sigma, t) = \varepsilon_0 + At^n = (\mu_1\sigma + \mu_2\sigma^2 + \mu_3\sigma^3) + (\gamma_1\sigma + \gamma_2\sigma^2 + \gamma_3\sigma^3)t^n. \quad (28)$$

Here, $\varepsilon(\sigma, t)$ is the creep strain spectrum. μ_i, γ_i and n representing seven fitting parameters. σ is the applied constant stress. Notably, early researchers recognized stress-dependence in creep strain/compliance, and characterizing strongly nonlinear creep compliance distributions marked a significant advancement [16–18]. However, power-law creep models and Nutting’s law inherently predict unbounded strain growth at all stress levels, directly conflicting with experimental observations of low-stress creep stabilization of viscoelastic solids. The power-law creep equation, widely used in rheology, is well-suited for characterizing non-Newtonian and creep-unstable fluid behaviors.

As the founder of biomechanics, Fung [37] developed the quasi-linear viscoelasticity (QLV) theory, which balances complexity and practicality in modeling biological soft tissue mechanics via a "quasi-linear" architecture. This framework has become a cornerstone in biomechanics, with its core principle decoupling nonlinear elasticity from linear viscoelasticity. The elastic stress $\sigma^e(\varepsilon)$ is nonlinear (such as an exponential function or polynomial), while the viscoelastic response is coupled with the elastic part through linear integration (convolution), forming a "quasi-linear" structure (Fig. 15). However, QLV theory is based on normalized relaxation modulus "G(t)". QLV theory exhibits limitations in characterizing strongly nonlinear viscoelasticity, as demonstrated by PP experimental results. Here, relaxation modulus decreases with increasing constant strain (Fig. 5a), indicating strain-dependent relaxation modulus spectrum $G(\varepsilon, t)$. QLV’s reliance on strain-independent inherently restricts its ability to capture such nonlinear viscoelastic behavior.

Schapery [39,68] extended linear viscoelasticity by introducing nonlinear correction functions and time-temperature superposition (shift factor), systematically deriving nonlinear viscoelastic constitutive equations (Fig. 16). This framework has found broad applications in polymers and their fiber-reinforced composites [69–71]. Notably, Rafiee et al. [69] developed a comprehensive integrated framework for creep analysis of composite structures incorporating the Schapery model, yielding significant advancements in predictive capabilities. Through inclusion of nonlinear correction functions (g_0, g_1, g_2, a_σ) and the

reduction time $\xi(t) = \int_0^t \frac{1}{a_\sigma(\sigma)} d\tau$ in this equation, the Schapery equation

achieves exceptional mathematical accuracy [68]. Notwithstanding, this formulation represents a mathematical correction, preserving instantaneous elastic compliance (D_0) or modulus (E_0) at the physical level (Fig. 16). Describe the instantaneous nonlinear elastic behavior through mathematical nonlinear functions g_0 and h_0 . Numerous visco-hyperelastic constitutive modeling systems have abandoned instantaneous elastic modulus and adopted instantaneous hyperelastic models to characterize instantaneous nonlinear elastic behavior. For example, constitutive modeling of hydrogels [60,61]. From a mechanistic perspective, Schapery’s equations resemble Kepler’s third law—a geometrically significant mathematical descriptor—while physical theories like Newtonian gravitation offer causal explanations. This essential distinction highlights that the Schapery model’s core value resides in its mathematical analysis framework for nonlinear corrections, rather than explanations of material mechanics principles.

Our research methodology diverges from Fung and Schapery’s equation-based corrections. Zhou et al. [24] introduced the "anchored" physical concept, systematically reframing the Boltzmann superposition principle. This work provides a quantitative formulation rooted in the Boltzmann nonlinear superposition principle, first establishing the dialectical unity between linear and nonlinear theories. Geometrically, a curve’s finite radius of curvature contrasts with a straight line’s infinite radius. In essence, a straight line represents a curve with an infinitely large radius, rendering it a limiting case of curved geometry. Similarly, instantaneous/infinite linear elastic behavior (straight line, Fig. 9a) and hyperelastic behavior (curve, Fig. 9b) exhibit analogous dialectical relationships, with linear viscoelasticity serving as the infinite limit of nonlinear viscoelasticity. Notably, nonlinear superposition constitutive relations exhibit broader applicability compared to their linear superposition constitutive relations. In nonlinear superposition, $J(\sigma_1, t) \neq J(\sigma_2, t) \neq J(\sigma_3, t)$ (Fig. 5b). In linear superposition, the nonlinear viscoelastic creep compliance spectrum can be simplified as linear viscoelastic creep compliance $J(\sigma_1, t) = J(\sigma_2, t) = J(\sigma_3, t) = J(t)$. This reduces Boltzmann nonlinear superposition equations to linear form (Fig. 16), demonstrating that the stress-independent linear principle represents a special case of stress-dependent nonlinear superposition. Theoretical analysis further reveals that the Boltzmann nonlinear superposition principle is applicable to anisotropic nonlinear viscoelastic materials [72].

Our key contribution is deriving the constitutive equations for single physical field superposition in nonlinear viscoelastic solids based on the

Boltzmann nonlinear superposition principle [24]. This nonlinear superposition framework exhibits profound dialectical coherence with the linear theoretical system. The derived equations bridge special statics (Fig. 1a) and generalized statics (Fig. 1b) of nonlinear viscoelastic materials, establishing a unified theoretical foundation for their mechanical behavior.

7. Conclusions

This study takes polypropylene as a typical nonlinear viscoelastic solid material and investigates its isotropic nonlinear viscoelastic properties. The main conclusions are as follows:

We propose and validate a general constitutive behavior framework for nonlinear viscoelastic solids, demonstrating that the infinite hyperelastic-plastic limit serves as the unique physical boundary governing structural creep stability. Our principal contribution lies in quantifying the threshold stress separating low-stress creep stability from high-stress creep instability—a critical improvement transitioning from qualitative to quantitative analysis.

We introduce a series-parallel theoretical framework of hyperelastic springs and dampers to characterize nonlinear viscoelasticity. Preliminary validation confirms the effectiveness of Maxwell-Mooney-Rivlin fluid relaxation and Kelvin-Mooney-Rivlin solid creep models. This architecture lays a foundational basis for future developments, including Maxwell-Ogden fluid relaxation and Kelvin-Blatz-Ko solid creep models, etc.

To predict material behavior under complex stress conditions, we derive Boltzmann's equations based on the nonlinear superposition principle, characterizing single-physics superposition in nonlinear viscoelastic solids. While Boltzmann's original work established linear

superposition relations, our innovation extends this to stress (strain)-dependent nonlinear superposition. Theoretical significance resides in the proposed methodology for constructing nonlinear viscoelastic theory systems, offering a scalable approach to future modeling challenges.

CRedit authorship contribution statement

Jinlai Zhou: Writing – review & editing, Writing – original draft, Visualization, Validation, Software, Resources, Project administration, Methodology, Investigation, Formal analysis, Data curation, Conceptualization. **Gengchao Yang:** Writing – review & editing, Supervision. **Qinghe Yao:** Writing – review & editing, Supervision, Funding acquisition.

Declaration of competing interest

The authors declare no competing financial interests.

Acknowledgement

This work has been supported by the National Natural Science Foundation of China (NSFC) under Grant No. 11972384, the Guangdong Basic and Applied Basic Research Foundation - Guangdong-Hong Kong-Macao Applied Mathematics Center Project under Grant No. 2021B1515310001, and the Guangdong Basic and Applied Basic Research Foundation - Regional Joint Fund Key Project under Grant No. 2022B1515120009. Additionally, we extend our appreciation to the National Key Research and Development Program under Grant No. 2020YFA0712502 for their invaluable support in this research.

Appendix A. Matrix form of the Mooney-Rivlin model

The incompressible isotropic Mooney Rivlin hyperelastic model is shown in Eq. (A1):

$$W = C_{10}(I_1 - 3) + C_{01}(I_2 - 3). \quad (\text{A1})$$

Due to the description of small deformations ($\epsilon < 5\%$). This study adopts the isotropic Cauchy stress-strain tensor measurement method. I_1 and I_2 are the first and second invariants of the Cauchy strain tensor. As shown in Eq. (A2):

$$\begin{cases} I_1 = \epsilon_{11} + \epsilon_{22} + \epsilon_{33} = 0 \text{ (incompressible)}. \\ I_2 = \epsilon_{11} \cdot \epsilon_{22} + \epsilon_{22} \cdot \epsilon_{33} + \epsilon_{33} \cdot \epsilon_{11} - (\epsilon_{12}^2 + \epsilon_{13}^2 + \epsilon_{23}^2). \end{cases} \quad (\text{A2})$$

Through principal direction analysis, complex three-dimensional problems can be transformed into independent deformation problems along the main axis, significantly reducing computational difficulty while preserving core physical mechanisms. Tensors degenerate into diagonal form, and invariants are directly calculated from principal values. This series of simplifications is aimed at allowing the nonlinear creep equation to be described using explicit equations.

The strain tensor invariant is simplified as the main strain tensor invariant, as shown in the Eq. (A3):

$$\begin{cases} I_1 = \epsilon_{11} + \epsilon_{22} + \epsilon_{33} = 0. \\ I_2 = \epsilon_{11} \cdot \epsilon_{22} + \epsilon_{22} \cdot \epsilon_{33} + \epsilon_{33} \cdot \epsilon_{11}. \end{cases} \quad (\text{A3})$$

The stress tensor is obtained by taking the partial derivative of the strain energy W with respect to the strain tensor, as shown in Eqs (A4) and (1b):

$$[\sigma_{ij}] = \left[\frac{\partial W}{\partial \epsilon_{ij}} \right] [\epsilon_{ij}]. \quad (\text{A4})$$

Data availability

Data will be made available on request.

References

- [1] Meyers MA, Chawla KK. *Mechanical behavior of materials*. (Cambridge Univ. Press); 2008.
- [2] Maxwell J C. On the dynamical theory of gases. *Philosoph Trans R Soc London* 1867;157:49–88.
- [3] Boltzmann L. Zur Theorie der elastischen Nachwirkung. *Sitzungsberichte der Kaiserlichen Akademie der Wissenschaften, Mathematisch-Naturwissenschaftliche Classe* 1874;70:275–306.
- [4] Markovitz H. Boltzmann and the beginnings of linear viscoelasticity. *Trans Soc Rheol* 1977;21:381–98.
- [5] Zhou J, Peng B, Yao Q, Yang G. Predicting delayed stability of metals at constant high temperatures. *Mat Sci Eng A-Struct* 2025;931(7620):148163.
- [6] Treloar L. The elasticity of a network of long-chain molecules—II. *Trans Faraday Soc* 1943;39:241–6.

- [7] Mooney M. A theory of large elastic deformation. *J Appl Phys* 1940.
- [8] Rivlin RS. Large elastic deformations of isotropic materials. *Philosoph Trans R Soc London* 1948.
- [9] Blatz PJ, Ko W. Application of finite elastic theory to the deformation of rubbery materials. *J Rheol* 1962;6(1):223–52.
- [10] Varga OH. Stress-strain behavior of elastic materials; selected problems of large deformations. New York: Wiley; 1966.
- [11] Veronda DR, Westmann RA. Mechanical characterization of skin—finite deformations. *J Biomech* 1970;3(1):111–24.
- [12] Ogden RW. Large deformation isotropic elasticity: on the correlation of theory and experiment for compressible rubberlike solids. *Proc Roy Soc London Series A* 1972; 326(2):565.
- [13] Arruda EM, Boyce MC. A three-dimensional constitutive model for the large stretch behavior of rubber elastic materials. *J Mech Phys Solids* 1993;41(2):389–412.
- [14] Yeoh OH. Some forms of the strain energy function for rubber. *Rubber Chem Technol* 1993;66(5):754–71.
- [15] Gent AN. A new constitutive relation for rubber. *Rubber Chem Technol* 1996;69(1):59–61.
- [16] Zhou J, Song Y, Shi X, Zhang C. Tensile creep mechanical behavior of periodontal ligament: A hyper-viscoelastic constitutive model. *Comput Meth Prog Bio* 2021; 207:106224.
- [17] Gao L, Zhang C, Gao H, Liu Z, Xiao P. Depth and rate dependent mechanical behaviors for articular cartilage: Experiments and theoretical predictions. *Mat Sci Eng C-Mater* 2014;38:244–51.
- [18] Gao L, Wei C, Zhang C, Gao H, Yang N, Dong L. Quasi-static and ratcheting properties of trabecular bone under uniaxial and cyclic compression. *Mat Sci Eng C-Mater* 2017;77:1050–9.
- [19] Peng GJ, Ma Y, Feng YH, Huan Y, Qin CJ, Zhang TH. Nanoindentation creep of nonlinear viscoelastic polypropylene. *Polym Test* 2015;43:38–43.
- [20] Rafiee R, Ghorbanhosseini A. Analyzing the long-term creep behavior of composite pipes: Developing an alternative scenario of short-term multi-stage loading test. *Compos Struct* 2020;254(9–10):112868.
- [21] Rafiee R, Mazhari B. Evaluating long-term performance of glass fiber reinforced plastic pipes subjected to internal pressure. *Constr Build Mater* 2016;122:694–701.
- [22] Rafiee R, Ghorbanhosseini A. Developing a micro-macromechanical approach for evaluating long-term creep in composite cylinders. *Thin Wall Struct* 2020;151: 106714.
- [23] Rafiee R, Ghorbanhosseini A. Experimental and theoretical investigations of creep on a composite pipe under compressive transverse loading. *Fiber. Polym* 2021;22: 222–30.
- [24] Zhou J, Tan Y, Song Y, Shi X, Lian X, Zhang C. Viscoelastic mechanical behavior of periodontal ligament: Creep and relaxation hyper-viscoelastic constitutive models. *Mech Mater* 2021;163:104079.
- [25] Rivlin RS, Ericksen JL. Stress-deformation relations for isotropic materials. *J Ration Mech Anal* 1955;4(6):323–425.
- [26] Rivlin RS. Nonlinear viscoelastic solids. *SIAM Rev* 1965;7(3):323–40.
- [27] Pipkin A. Small finite deformations of viscoelastic solids. *Rev Modern Phys* 1964; 36(4):1034.
- [28] Pipkin A, Rogers T. A non-linear integral representation for viscoelastic behaviour. *J Mech Phys Solids* 1968;16(1):59–72.
- [29] Green AE, Rivlin RS. The mechanics of non-linear materials with memory I. *Arch Ration Mech Anal* 1957;1(1):1–21.
- [30] Green AE, Rivlin RS. The mechanics of non-linear materials with memory III. *Arch Ration Mech Anal* 1959;4:387–404.
- [31] Green AE, Rivlin RS, Spencer AJM. The mechanics of non-linear materials with memory II. *Arch Ration Mech Anal* 1959;3:82–90.
- [32] Wang CC. The principle of fading memory. *Arch Ration Mech Anal* 1965;18: 343–66.
- [33] Findley J, Lai JS, Onaran K. Creep and relaxation of nonlinear viscoelastic materials. North-Holland Pub Co; 1976.
- [34] Onaran K, Findley WN. Combined stress-creep experiments on a nonlinear viscoelastic material to determine the kernel functions for a multiple integral representation of creep. *J Rheol* 1965;9(2):299–327.
- [35] Lai JSY, Findley WN. Prediction of uniaxial stress relaxation from creep of nonlinear viscoelastic material. *J Rheol* 1968;12(2):243–57.
- [36] Ward IM, Onat ET. Non-linear mechanical behaviour of oriented polypropylene. *J Mech Phys Solids* 1963;11(4):217–29.
- [37] Fung YC. Stress-strain history relations of soft tissues in simple elongation. *J Biomech* 1972;5(5):531–42.
- [38] Fung YC. *Biomechanics: mechanical properties of living tissues*. New York: Springer; 1981.
- [39] Schapery RA. A theory of nonlinear thermoviscoelasticity based on irreversible thermodynamics. *Proceedings of the fifth US national congress of applied mechanics*. Minnesota: University of Minnesota; 1966. p. 511–30.
- [40] Amabili M. Nonlinear damping in nonlinear vibrations of rectangular plates: derivation from viscoelasticity and experimental validation. *J Mech Phys Solids* 2018;118:275–92.
- [41] Yang TQ. *Viscoelastic mechanics*. Wu Han: Huazhong University of Science and Technology Press; 1990.
- [42] Urbach E, Efrati E. Predicting delayed instabilities in viscoelastic solids. *Sci Adv* 2020;6(36).
- [43] Huo M, Yu Y, Xia R, Xu J. A new creep constitutive relationship for high temperature alloys. *Int J Mech Sci* 2021;194(2):106207.
- [44] Tao K, Khonik VA, Qiao JC. Indentation creep dynamics in metallic glasses under different structural states. *Int J Mech Sci* 2023;240(5817):107941.
- [45] Zhang C, Zhang T, Gao L, Du C, Liu Q, Liu H, Wang X. Ratcheting Behavior of Intervertebral Discs Under Cyclic Compression: Experiment and rediction. *Orthopaedic Surgery*; 2019;11:895–902.
- [46] Wang M, Liu S, Xu Z, Qu K, Li M, Chen X, Xue Q, Genin G, Lu T, Xu F. Characterizing poroelasticity of biological tissues by spherical indentation: An improved theory for large relaxation. *J Mech Phys Solids* 2020;138:103920.
- [47] Lovrenić-Jugović M, Tonković Z, Skozrit I. Experimental and numerical investigation of cyclic creep and recovery behavior of bovine cortical bone. *Mech Mater* 2020;146:103407.
- [48] Pedoto G, Grandidier J, Gigliotti M, Vinet A. Characterization and modelling of the PEKK thermomechanical and creep behavior above the glass transition temperature. *Mech Mater* 2022;166(2):104189.
- [49] Cui Y, Campbell J, burley M, Patel M, Hunt K, Clyne T. Effects of temperature and filler content on the creep behaviour of a polyurethane rubber. *Mech Mater* 2020; 148(1):103461.
- [50] Mazurek G. Effect of filler type on non-linear viscoelastic characteristics of asphalt mastic. *Arch Civ Eng* 2021;67:247–59.
- [51] Wu F, Zhang H, Zou Q, Li C, Chen J, Gao R. Viscoelastic-plastic damage creep model for salt rock based on fractional derivative theory. *Mech Mater* 2020;150: 103600.
- [52] Cao P, Short M, Yip S. Understanding the mechanisms of amorphous creep through molecular simulation. *P Natl Acad Sci USA* 2017;114(52):201708618.
- [53] Zhou J, Song Y, Shi X, et al. Experimental research on viscoelasticity property of different layers periodontal ligament under compression. *J Mech Med Biol* 2022;22(01):2150050.
- [54] Goudoulas TB, Germann N. Viscoelastic properties of polyacrylamide solutions from creep ringing data. *J Rheol* 2016;60(3):491–502.
- [55] Tassieri M, Waigh TA, Trinick J, Aggeli A, Evans RML. Analysis of the linear viscoelasticity of polyelectrolytes by magnetic microrheometry—pulsed creep experiments and the one particle response. *J Rheol* 2010;54(1):117–31.
- [56] Jamshidi M, Shokrieh M. On the Schapery nonlinear viscoelastic model: A review. *Eur J Mech A-Solid* 2024;108:105403.
- [57] Loy RJ, de Hoog Fr RS, Anderssen RS. Interconversion of Prony series for relaxation and creep. *J Rheol* 2015;59(5):1261–70.
- [58] Xiang Y, Zhong D, Wang P, Mao G, Yu H, Qu S. A general constitutive model of soft elastomers. *J Mech Phys Solids* 2018;117:110–22.
- [59] Xiang Y, Zhong D, Wang P, Yin T, Zhou H, Yu H, Baliga C, Qu S, Yang W. A physically based visco-hyperelastic constitutive model for soft materials. *J Mech Phys Solids* 2019;128:208–18.
- [60] Zhong D, Xiang Y, Wang Z, Chen Z, Liu J, Wu Z, Xiao R, Qu S, Yang W. A visco-hyperelastic model for hydrogels with tunable water content. *J Mech Phys Solids* 2023;173:105206.
- [61] Wang Z, Zhong D, Xiao R, Qu S. Correlation between synthesis parameters and hyperelasticity of hydrogels: Experimental investigation and theoretical modeling. *J Mech Phys Solids* 2024;190:105733.
- [62] Flory PJ. Thermodynamic relations for high elastic polymers. *Trans Faraday Soc* 1961;57:829–38.
- [63] Zhao Y. *Modern continuum mechanics*. Science Press; 2016.
- [64] Hibbitt D, Karlsson B, Sorensen P. *ABAQUS/standard user's manual*. USA: HKS Inc; 2010.
- [65] Pellicciari M, Sirotti S, Tarantino A. A strain energy function for large deformations of compressible elastomers. *J Mech Phys Solids* 2023;176(4):105308.
- [66] Nutting PG. *Proc. ASTM* 1921;21:1162–71.
- [67] Rees DWA. Nutting creep in polymer composites. *J Mater Process Tech* 2003: 164–70.
- [68] Jamshidi M, Shokrieh MM. On the Schapery nonlinear viscoelastic model: a review. *Eur J Mech A-Solid* 2024;108(4):105403.
- [69] Rafiee R, Mazhari B. Modeling creep in polymeric composites: developing a general integrated procedure. *Int J Mech Sci* 2015;99:112–20.
- [70] Yu C, Kang G, Lu F, Zhu Y, Chen K. Viscoelastic-viscoplastic cyclic deformation of polycarbonate polymer: experiment and constitutive model. *J Appl Mech* 2016;83(4):041002.
- [71] Zink T, Kehrer L, Hirschberg V, Wilhelm M, Böhlke T. Nonlinear Schapery viscoelastic material model for thermoplastic polymers. *J Appl Polym Sci* 2022; 139:52028.
- [72] Sadik S, Yavari A. Nonlinear anisotropic viscoelasticity. *J Mech Phys Solids* 2024; 182:105461.